

1
2
3
4
5
6 **A New Tropical Savanna PFT, Variable Root Growth and Fire Improve Cerrado**
7 **Vegetation Dynamics Simulations in a Dynamic Global Vegetation Model**
8

9 Jéssica Schüler^{1,2*}, Sarah Bereswill^{2*}, Werner von Bloh²,
10 Maik Billing², Boris Sakschewski², Luke Oberhagemann^{2,3}, Kirsten Thonicke² and
11 Mercedes M.C. Bustamante¹

12
13 ¹ Department of Ecology, University of Brasília, Campus Universitário Darcy Ribeiro,
14 70910-900, Brasília, Brazil

15 ² Potsdam Institute for Climate Impact Research, Telegrafenberg A 31, 14473 Potsdam,
16 Germany

17 ³ Institute of Environmental Science and Geography, University of Potsdam, Karl-
18 Liebknecht Str. 24/25, Potsdam, Germany

19
20 *Correspondence to:* Jéssica Schüler (jehschuler@gmail.com)

21 **Abstract**

22 The Cerrado, South America's second largest biome, has been historically
23 underrepresented in Dynamic Global Vegetation Models (DGVMs). Therefore, this study
24 introduces a novel Plant Functional Type (PFT) tailored to the Cerrado biome into the
25 DGVM LPJmL-VR-SPITFIRE. The parametrization of the new PFT, called a Tropical
26 Broadleaved Savanna tree (TrBS), integrates key ecological traits of Cerrado trees,
27 including specific allometric relationships, wood density, specific leaf area (SLA), deep-
28 rooting strategies, and fire-adaptive characteristics. The inclusion of TrBS in LPJmL-VR-
29 SPITFIRE led to notable improvements in simulated vegetation distribution. TrBS became
30 dominant across Brazil's savanna regions, particularly in the Cerrado and Pantanal. The
31 model also better reproduced the above- and belowground biomass patterns, accurately
32 reflecting the "inverted forest" structure of the Cerrado, characterized by a substantial
33 investment in root systems. Moreover, the presence of TrBS improved the simulation of
34 fire dynamics, increasing estimates of burned area and yielding seasonal fire patterns more
35 consistent with observational data. Model validation confirmed the enhanced performance
36 of the model with the new PFT in capturing vegetation structure and fire regimes in Brazil.
37 Additionally, a global-scale test demonstrated reasonable alignment between the simulated
38 and observed global distribution of savannas. In summary, the integration of the TrBS PFT
39 marks a critical advancement for LPJmL-VR-SPITFIRE, offering a more robust
40 framework for investigating the interaction of above- with belowground ecological
41 processes, fire disturbance and the impacts of climate change across the Cerrado and other
42 tropical savanna ecosystems that together account for approximately 30 % of the primary
43 production of all terrestrial vegetation.

44

45 **1. Introduction**

46 Brazil spans over 850 million hectares, from approximately 5°N to 35°S, and hosts
47 diverse climatic conditions, from subtropical and semi-arid to tropical wet environments
48 (IBGE, 2024; Table S1). Within this context, the Cerrado is recognized as the world's most
49 biodiverse savanna and the second-largest vegetation formation in South America,
50 covering about 23% of Brazil (~2 million km²), mainly in the central region (Myers et al.,
51 2000; IBGE, 2024). The biome provides vital ecosystem services, including carbon
52 storage, climate regulation, and water resources for major river basins (Sano et al., 2019;
53 Schüler & Bustamante, 2022). Despite its global importance, the Cerrado faces severe
54 threats from deforestation driven by agricultural expansion and from climate change,
55 which is intensifying droughts and altering fire regimes, thereby accelerating biodiversity
56 loss and ecosystem degradation (Strassburg et al., 2017; Gomes et al., 2020a; Rodrigues
57 et al., 2022). ~~The Cerrado, a biome of global importance and recognized as the world's most~~
58 ~~biodiverse savanna, faces numerous challenges that threaten its rich biodiversity and the~~
59 ~~vital ecosystem services it provides (Myers et al., 2000; Sano et al., 2019; Schüler and~~
60 ~~Bustamante, 2022).~~ The alarming deforestation rates, driven by agricultural expansion, and
61 ~~the impacts of climate change, which are already exacerbating droughts and altering fire~~
62 ~~dynamics, are the two main drivers of degradation, impacting water availability and~~
63 ~~vegetation dynamics in this biome (Strassburg et al., 2017; Gomes, et al., 2020a; Rodrigues~~
64 ~~et al., 2022).~~

65 Climate change impacts in Brazil are already evident. A study by INPE to the First
66 Biennial Transparency Report (MCTI, 2024) reveals an increase of approximately 20% in
67 the number of consecutive dry days in Brazil in recent decades, particularly in the North,
68 Northeast, and Central regions of the country. Similarly, Feron et al., (2024) demonstrated
69 an increase in the frequency of compound climate events involving heat, drought, and high

70 fire risk in key regions of South America, including the Amazon. A significant increase in
71 maximum and minimum temperatures was also observed in the Brazilian Cerrado between
72 1961 and 2019, along with a reduction in relative humidity (Hofmann et al., 2021).

73 In this context, vegetation modeling emerges as an essential tool for understanding and
74 predicting the Cerrado's responses to these pressures. Dynamic Global Vegetation Models
75 (DGVMs), such as the Lund-Potsdam-Jena managed Land model (LPJmL), aim to
76 simulate changes in vegetation, fire, water and carbon fluxes depending on climate and
77 land use (Cramer et al., 2001; Thonicke et al., 2010; Baudena et al., 2015; Moncrieff et al.,
78 2016; Schaphoff et al., 2018; Drüke et al., 2019; Martens et al., 2021). In order to reduce
79 complexity, common DGVMs classify vegetation into so-called Plant Functional Types
80 (PFTs), which are groups of plants that show similar responses to external drivers and
81 resemble their ecological function. PFTs are, in general, distinguished by their allometry,
82 growth form, phenology and photosynthetic strategy (Wullschleger et al., 2014).
83 Parameterization of PFTs should therefore capture the most important characteristics of
84 certain vegetation types while balancing complexity.

85 Specifically in savannas, vegetation is often characterized by small trees and shrubs that
86 grow deep roots and are well adapted to fire and drought, all of which distinguish them
87 from the trees in moist and seasonal tropical forests (Ratnam et al., 2011). However, many
88 DGVMs, including LPJmL, lack a dedicated savanna PFT, leading to significant
89 inconsistencies in model projections (Foley et al., 1998; Hughes, Valdes and Betts, 2006;
90 Clark et al., 2011; Neilson, R. P. 2015; Drüke; et al., 2019). This omission often results in
91 the underestimation of savanna vegetation extent and fire occurrences, while
92 overestimating above-ground biomass and the extent of tall tropical forest formations, as
93 demonstrated in simulations for South America (Cramer et al., 2001; Drüke et al., 2019),
94 or a depiction of savanna vegetation as tropical grasslands which do not encompass the

95 coexistence of grasses, shrubs and trees. DGVMs are, nevertheless, widely used to
96 simulate future transitions between the Amazon and the Cerrado biomes, often predicting
97 an abrupt shift from forest to grassland under climate change (Malhi et al., 2009; Swann
98 et al., 2015). However, this oversimplification neglects the intricate ecological gradient
99 that spans diverse vegetation types, from open forests to woody savannas with varying tree
100 cover densities.

101 This lack of precision in modeling has broader implications for understanding the
102 Cerrado's role in climate mitigation and adaptation, including nature restoration. For
103 example, restoring the entire 20 million hectares of the identified priority areas for
104 restoration in the Cerrado could remove up to 1.77 million tons of carbon from the
105 atmosphere (Schüler and Bustamante, 2022). Beyond carbon sequestration, savannas play
106 a crucial role in preserving water resources and biodiversity, acting as natural buffers
107 against climate change and enhancing ecosystem resilience (Oliver et al., 2015; Salazar et
108 al., 2016; Syktus and McAlpine 2016; Bustamante et al., 2019). With its highly seasonal
109 climate and diverse mosaic of grasslands, savannas, and forest formations, the Cerrado is
110 particularly significant for mitigating and adapting to climate change (Ribeiro and Walter
111 2008; Bustamante et al., 2019; Schüler and Bustamante 2022). Accurately representing
112 savanna-type vegetation in DGVMs will not only improve projections of the Cerrado's
113 vulnerability to climate change but also help identify high-risk areas and guide the
114 development of effective conservation, restoration, and management strategies. For
115 instance, improved models, acknowledging savanna-specific characteristics, could inform
116 studies investigating biome transitions and ecological tipping points, fire management
117 measures, support agricultural adaptation, and optimize water resource management,
118 ensuring the Cerrado's resilience in the face of environmental challenges.

119 We therefore introduce a new Cerrado specific PFT which we call “Tropical
120 Broadleaved Savanna tree”^e (TrBS) that entails the biome's unique characteristics into a
121 state-of-the-art version of the LPJmL model (LPJmL-VR-SPITFIRE). LPJmL-VR-
122 SPITFIRE explicitly simulates variable tree rooting strategies (Sakschewski et al., 2021)
123 and employs the process-based fire model SPITFIRE (Thonicke et al., 2010;
124 Oberhagemann et al., 2025), while being based on the latest LPJmL version (LPJmL 5.7;
125 Wirth et al., 2024). In this study, we test our new approach by modeling the Potential
126 Natural Vegetation (PNV) distribution for the entire Brazil and validate our results against
127 observational datasets. This model improvement provides a robust basis for studies
128 exploring the impact of climate change on vegetation dynamics in the Cerrado region. This
129 model is expected to show significant improvements in biomass estimate, vegetation type
130 distributions, and fire dynamics in tropical regions.

131 **2. Methods**

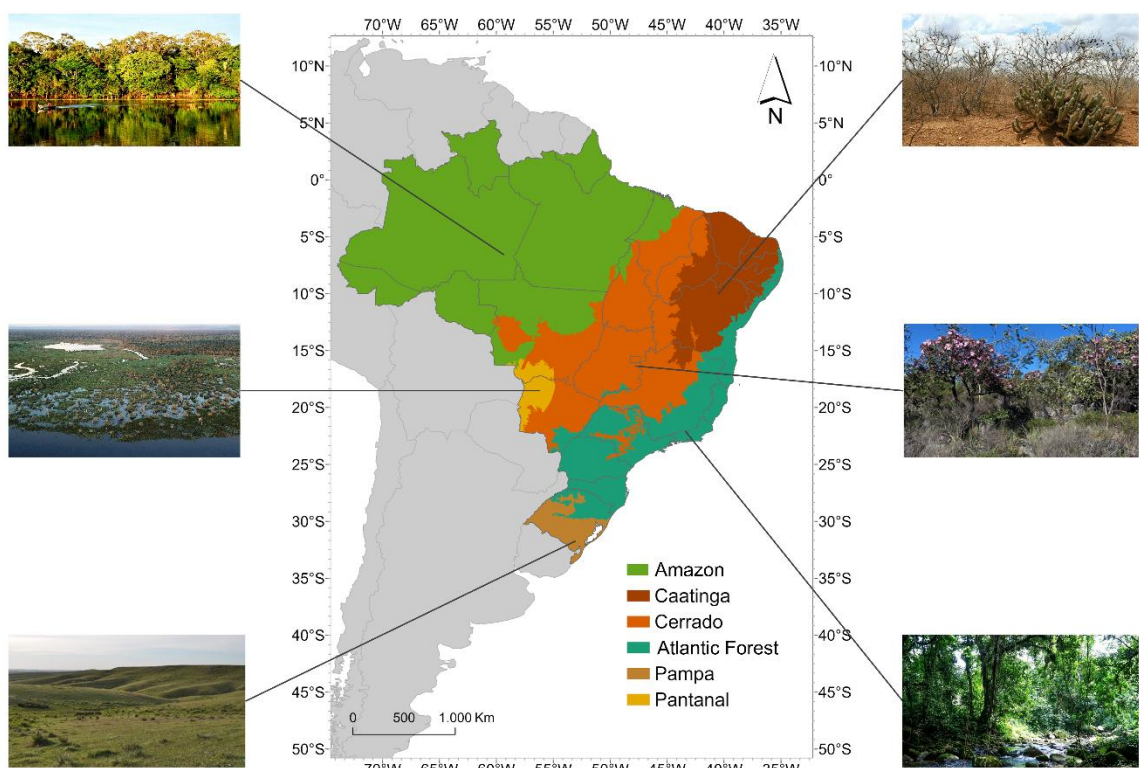
132 ***2.1 Study region***

133 Our study region encompasses all of the Brazilian territory, focusing on the distribution
134 of its six biomes, with special attention to the Cerrado biome. Because of its central
135 position, the Cerrado has ecotones with four of the other five Brazilian biomes: Amazon,
136 Caatinga, Atlantic Forest and Pantanal (Fig. 1).

137 ~~Brazil spans over 850 million hectares, extending from approximately 5°N to 35°S~~
138 ~~(IBGE, 2024). Due to its size, the country encompasses a wide range of climatic~~
139 ~~conditions, from subtropical and semi-arid regions to tropical wet environments (Table~~
140 ~~S1). The Cerrado, the second largest vegetation formation in South America, covers about~~
141 ~~23% of Brazil (~2 million km²), primarily in its central region (IBGE, 2024).~~ Recognized
142 as both a savanna and a global biodiversity hotspot, Cerrado's seasonal precipitation
143 regime is closely tied to the South American Monsoon System (Myers et al., 2000; Grimm,

144 Vera and Mechoso, 2004). ~~Its climate is predominantly classified as tropical savanna (Aw)~~
145 ~~according to the Köppen-Geiger classification system, characterized by a rainy season~~
146 ~~from October to April and a dry season from May to September. According to the Köppen-~~
147 ~~Geiger classification, the region's climate is predominantly tropical savanna (Aw) with a~~
148 ~~rainy season from October to April and a dry season from May to September.~~ (Peel et al.,
149 2007; Oliveira et al., 2021). Annual rainfall ranges from 600 mm to 2,000 mm, with the
150 highest averages near the Amazon border and the lowest near the Caatinga, and the mean
151 annual temperature is 20.1°C (Sano et al., 2019).

152



153
154 Fig. 1: Map representing the distribution of Brazilian biomes according to IBGE (2024)
155 and photos showing their general appearances. Amazon photo by Andre Deak, Pantanal
156 photo by Leandro de Almeida Luciano, Pampa photo by Ilsi Boldrini, Caatinga photo by
157 Matheus Andrietta, Cerrado photo by Jéssica Schüler, and Atlantic Forest photo by Tânia
158 Rego.

159

160 Historically, the biome is subject to periodic fires, especially in the grassland and
161 savanna formations, highly influencing the evolution of its vegetation (Simon et al., 2009;
162 Simon and Pennington 2012). Currently, fires predominantly occur at the end of the dry
163 season, during September and October (Gomes et al., 2020; MapBiomas Fogo 2024). The
164 vegetation in the Cerrado can be classified into three main vegetation formations: Forests,
165 Savannas and Grasslands. ~~Forested~~ formations predominantly consist of trees forming a
166 continuous canopy, typically found on deeper soils (Ribeiro and Walter 2008). Savanna
167 formations are defined by the presence of both arboreal and herbaceous-shrub strata with
168 a canopy cover ranging from 5% to 70% and tree heights reaching 8 m on average (Ribeiro
169 and Walter 2008). Finally, grassland formations consist of shrubs and sub-shrubs
170 intermixed with herbaceous strata (Ribeiro and Walter 2008).

171

172 ***2.2 Model description***

173 The LPJmL-VR-SPITFIRE model is a fire-enabled DGVM that integrates the latest
174 version of the DGVM LPJmL (LPJmL 5.7, Wirth et al., 2024) with the most recent
175 improvements of the SPITFIRE fire regime model (Thonicke et al., 2010; Oberhagemann
176 et al., 2025), together with the variable-roots (VR) developed by Sakschewski et al.,
177 (2021). This model framework enables the simulation of global vegetation dynamics,
178 including ~~the fire~~-influence ~~of~~-fire disturbance (Schaphoff et al., 2018; Drüke et al., 2019).

179 LPJmL simulates the growth and productivity of both natural and managed vegetation,
180 considering water, carbon, and energy fluxes, and represents vegetation through PFTs
181 (Schaphoff et al., 2018). The model accounts for factors such as climate, soil, water, and
182 nutrient availability to simulate the distribution, biomass, and productivity of PFTs, and
183 has been validated against observational data on productivity, biomass, evapotranspiration

184 and PFT distribution on the global scale (Schaphoff et al., 2018). We briefly outline only
185 the most important features of the LPJmL-VR-SPITFIRE model version, while referring
186 to Schaphoff et al., (2018) for the general LPJmL model description.

187 *Variable roots*: In the original LPJmL model, a PFT-specific shape parameter β defines
188 tree rooting depth and fine root biomass distribution (Jackson et al., 1996). To better reflect
189 the diversity of rooting strategies of tropical trees, Sakschewski et al., (2021) introduced a
190 range of possible rooting strategies (shallow to deep rooted trees) per PFT, that can coexist
191 or outcompete each other. Unless constrained physically by soil depth or by available
192 resources, actual rooting depth is scaled with tree height via a logistic root growth function,
193 and new carbon pools (root sapwood and heartwood) represent the plant's investment in
194 growing coarse roots (Sakschewski et al., 2021). A long-term selection of the best suited
195 rooting strategies amongst each PFT is mediated by a modified tree establishment
196 approach, where the most successful rooting strategies can produce more saplings.

197 *Water-stress mortality*: Tree mortality in LPJmL depends on tree longevity, growth
198 efficiency and heat stress (Schaphoff et al., 2018). In this study, a new mortality component
199 reflecting mortality risk due to water stress has been included. This newly integrated water
200 stress mortality depends on tree phenology (*phen*) (Forkel et al., 2014, applied in
201 Schaphoff et al., 2018), leaf senescence due to water stress (*phen_{water}*) and PFT-specific
202 parameters representing water stress resistance (c_{res}) and sensitivity to drought (c_{sens}).

203
$$mort_{water} = c_{sens} \cdot phen \cdot (1 - phen_{water} - c_{res}) \quad (1)$$

204 c_{sens} is a PFT-specific parameter that determines the overall sensitivity to drought stress.
205 *Phen* represents the actual phenological state of a tree, ranging from 0 (no leaf cover) to 1
206 (full leaf cover). This term accounts for the fact that trees with lower phenology (i.e., more
207 dormant trees) experience reduced water stress mortality. The expression $(1 - phen_{water})$
208 represents the intensity of leaf senescence due to low water availability (Forkel et al.,

209 2014), indicating that periods of reduced water availability lead to higher drought-induced
210 mortality. c_{res} defines a threshold below which drought-induced leaf senescence does not
211 significantly impact tree survival.

212 This model refinement allows for a more accurate representation of PFT-specific
213 sensitivity to water stress. Coupled with the variable rooting scheme, LPJmL-VR-
214 SPITFIRE allows trees to optimize the trade-off between carbon investment in deep roots
215 and aboveground growth, providing a survival advantage under drought conditions. The
216 PFT-specific parameters are found in Table 1.

217 *SPITFIRE* is a process-based fire model that simulates wildfire occurrence, spread, and
218 behavior, while considering fuel availability, fuel composition and weather conditions to
219 simulate ignitions, rate of spread and flame intensity (Thonicke et al., 2010). By coupling
220 SPITFIRE into LPJmL-VR (LPJmL-VR-SPITFIRE), SPITFIRE can simulate the
221 influence of fire on vegetation dynamics. Vegetation properties simulated by LPJmL-VR,
222 such as PFT composition and litter fuel moisture, determine the simulation of fire spread
223 and intensity which in turn influence post-fire vegetation conditions. SPITFIRE considers
224 both human-induced and natural ignitions, with the likelihood of these ignitions
225 developing into fires depending on the fire danger index of the modelled grid cell. Fires
226 then spread depending on factors such as dead and live fuel composition, wind speed, and
227 fuel moisture. We adopted the VPD (water vapor pressure deficit)-dependent calculation
228 of the fire danger index (Drücke et al., 2019; Gomes et al., 2020b) and the most recent
229 updates to the fire spread functions (Oberhagemann et al., 2025). Both the fire danger
230 index and rate of spread calculations include PFT-specific parameters that reflect different
231 vegetation related properties that affect ignition, fire duration and propagation. Fire-related
232 tree mortality is calculated considering PFT specific bark thickness (influencing cambial
233 damage) and scorch height (influencing crown mortality). Furthermore, with the recent

234 updates, SPITFIRE allows for multi-day fires and considers moisture of the live grass
235 share. SPITFIRE feeds back to the vegetation components by calculating fire effects on
236 the vegetation, such as fuel combustion and post-fire tree mortality (Drücke et al., 2019;
237 Oberhagemann et al., 2025).

238

239 ***2.3 Parameterization of a new Savanna tree PFT***

240 The Cerrado trees exhibit considerable morphological and physiological differences
241 compared to other tropical forest trees growing in closed canopy and wet environments. In
242 LPJmL, these forests are represented by the Tropical Broadleaved Evergreen Tree PFT
243 (TrBE), reflecting the Amazon and the Atlantic rainforests, and by the Tropical
244 Broadleaved Raingreen Tree PFT (TrBR), representing seasonal closed forests. In contrast,
245 Cerrado vegetation is shaped by allometric relationships, and traits such as wood density,
246 specific leaf area (SLA), rooting depth, and bark thickness, which together create a
247 distinctive vegetation structure and functioning highly adapted to seasonal drought and fire
248 occurrence. To incorporate these characteristics into the LPJmL-VR-SPITFIRE model, we
249 used a combination of literature data and field observations to derive and calibrate the
250 relevant parameters for the new Tropical Broadleaved Savanna tree (TrBS)
251 parametrization. A summary of all parameters and data sources used is provided in Table
252 1 and 2, with detailed explanations below. Tree functional traits such as allometry, wood
253 density, specific leaf area (SLA), rooting depth, bark thickness, among others, contribute
254 to a distinctive vegetation structure and functioning, which are highly adapted to periodic
255 drought and fire regimes. To incorporate these characteristics into the LPJmL-VR-
256 SPITFIRE model, we used a combination of literature data and field observations to derive
257 and calibrate the relevant parameters for the new Tropical Broadleaved Savanna tree

258 (TrBS) parametrization. A summary of all parameters and data sources used is provided in
259 Table 1 and 2, with detailed explanations below.

260 *2.3.1 Allometry and growth form*

261 The tree allometry is defined through a diameter distribution that follows an asymptotic
262 pattern, where height increases at a slower rate as diameter grows larger, with most trees
263 remaining under 10 meters in height (Fig. S2A and C). A similar trend is observed in the
264 relationship between diameter and crown area: trees initially grow in diameter,
265 subsequently expanding their crown until crown growth reaches a plateau (Fig. S2B and
266 D). This observed growth pattern is implemented by allometric relationships using PFT-
267 specific allometric parameters within the LPJmL model (Schaphoff et al., 2018; Eqn. S1;
268 Eqn. S2). To ensure an accurate representation of TrBS's tree growth, we analyzed field
269 data to estimate maximum height, maximum crown area, and their relationship with stem
270 diameter (Table S2). Using these field measurements, we derived the allometric constant
271 values that best aligned with the observed data, by fitting the allometric equations to the
272 data (Fig. S2). Details about site location, data collected, and their references can be found
273 on Table S2.

274 Despite variations of wood density and SLA due to factors such as soil quality,
275 temperature, and water availability, trees in more arid environments typically develop
276 denser wood with lower SLA values (indicating thicker leaves), an adaptation to water
277 scarcity and mechanical stress (Scholz et al., 2008; Terra et al., 2018, Souza et al., 2024).
278 While we based our wood density value on literature (Souza et al., 2024), the SLA values
279 used in the development of TrBS PFT were estimated from field data collected from 71
280 individuals of 26 species (Table 1, Table S2).

281

282 Table 1: Allometry, drought mortality and rooting parameters used to define the new
 283 Tropical Broadleaved Savanna Tree (TrBS) PFT, along with the corresponding values for
 284 the Tropical Broadleaved Evergreen Tree (TrBE), and Tropical Broadleaved Raingreen
 285 Tree (TrBR). References cited apply exclusively to TrBS PFT. Details about the field
 286 survey data are available on Table S2. Additional information on TrBE and TrBR
 287 parameters, as well as parameters not included in this table, can be found in Schaphoff et
 288 al., (2018).

Parameter	Tropical Broadleaved Evergreen tree	Tropical Broadleaved Raingreen tree	Tropical Broadleaved Savanna tree	Reference
<u>Specific Leaf Area (SLA)</u> (mm ² .mg ⁻¹)	9.04	14.71	7.36	Field survey (Table S2)
Wood density (g.cm ⁻³)	0.44	0.44	0.6	Souza et al., (2024)
Max. height (m)	100	100	10	Field survey (Table S2)
Max.crown area (m ²)	25	15	10	Field survey (Table S2)
Parameter in allometry function (K - <i>allom</i> 1)	100	100	153	Field survey (Table S2)
Parameter in allometry function (K - <i>allom</i> 2)	40	40	12	Field survey (Table S2)
Parameter in allometry function (K - <i>allom</i> 3)	0.67	0.67	0.52	Field survey (Table S2)

Parameter	Tropical Broadleaved Evergreen tree	Tropical Broadleaved Raingreen tree	Tropical Broadleaved Savanna tree	Reference
Maximum leaf-to-root-mass-ratio scaling parameter (lr_{max})	1	1	0.7	
Vertical root distribution parameter (β_{root})		[0.9418, 0.9851, 0.9925, 0.9950, 0.9963, 0.9971, 0.9976, 0.9981, 0.9986, 0.9993]		Sakschewski et al., (2021)
Shape parameter in logistic root growth function (k_{root})	0.02	0.02	0.07	Saboya and Borghetti (2012)

289

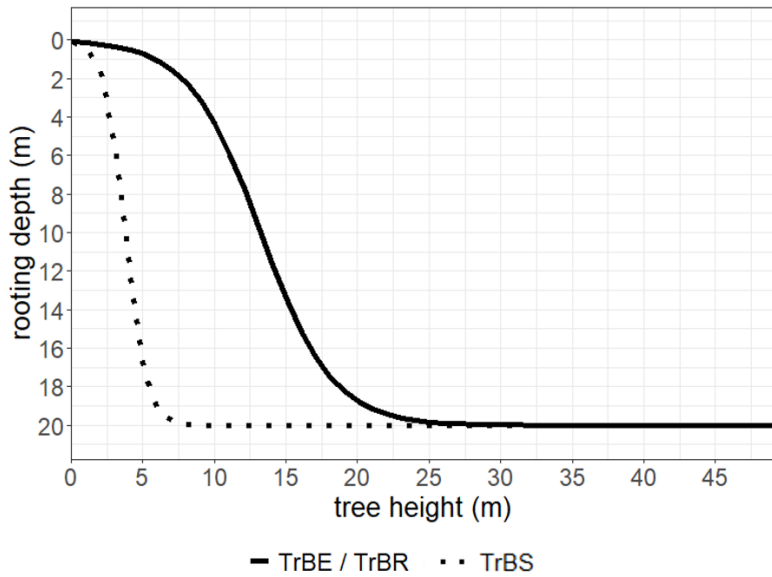
290 *2.3.2 Root growth and belowground carbon allocation*

291 Rooting depth is a crucial adaptation for the Cerrado species, enabling access to deep
 292 water reserves during prolonged dry periods (Oliveira et al., 2005; Tumber-Dávila et al.,
 293 2022). Due to its high investment in belowground structures, the Cerrado is often referred
 294 to as an 'upside-down forest,' storing approximately five times more carbon below-ground
 295 (in roots and as soil carbon) than above-ground (Terra et al., 2023). While deep roots are
 296 a well-documented feature of the Cerrado plants, rooting strategies vary widely among
 297 species. To try to reflect this diversity in rooting strategies in LPJmL-VR-SPITFIRE we
 298 allowed for 10 different root distributions (β_{root} parameter) per PFT. We chose the same
 299 range of β_{root} values for TrBS PFT as for the other PFTs, to allow a spectrum of shallow,
 300 intermediate and deep rooting strategies to compete. From β_{root} the depth where 95% of
 301 root biomass are found (D95) can be calculated (see Sakschewski et al., 2021). Studies
 302 show that the Cerrado tree seedlings invest more in root growth compared to shoot growth
 303 as a strategy to access water deeper in soil during the dry season (Hoffmann, Orthen and

304 Franco 2004; Saboya and Borghetti 2012). We reflect this by modifying the shape
305 parameter of the logistic root growth function (k_{root} , Table 1), to allow TrBS to reach
306 deeper rooting depths ~~already~~ earlier in their lifecycle (Fig. 2), enhancing the underground
307 competitiveness of these savanna trees. In LPJmL-VR-SPITFIRE, carbon allocation to
308 coarse woody roots is represented by separate root sapwood and heartwood carbon pools,
309 introduced in addition to the fine root carbon pool (Sakschewski et al., 2021). Due to the
310 necessary balance between root and stem sapwood investment (Pipe Model approach;
311 Shinosaki et al., 1964), and the relationship between tree height and rooting depth, deep
312 root growth for TrBS saplings represents a trade-off between above- and belowground
313 growth.

314 The ratio between the leaf and the fine root biomass in the model depends on the
315 model internally calculated water stress index (ω), where more root biomass is built
316 under water stress, and is constrained by the lr_{max} (maximum leaf-to-root-mass-ratio)
317 scaling parameter (Table 1; Schaphoff et al., 2018). We set lr_{max} to 0.7 to allow TrBS to
318 invest relatively more into root biomass than the other tropical tree PFTs, where lr_{max} was
319 set to 1 (Schaphoff et al., 2018).

320



321

322 Fig. 2: Logistic growth function scaling rooting depth to tree height, shown for a soil depth
 323 of 20m for the different PFTs (TrBE = tropical broadleaved evergreen, TrBR = tropical
 324 broadleaved raingreen, TrBS = Tropical Broadleaved Savanna).

325

326 *2.3.2 Phenology*

327 The Cerrado exhibits pronounced precipitation seasonality, which shapes the
 328 phenology of its vegetation. Deciduous and semi-deciduous species display leaf dynamics
 329 in which leaves shed during the dry season, peaking in July, and sprout during the
 330 transition to the rainy season in September (de Camargo et al., 2018). Despite the
 331 dominance of deciduous and semi-deciduous species (74%), the community rarely
 332 experiences complete defoliation, retaining at least half of its foliage in most years (de
 333 Camargo et al., 2018). This seasonal pattern is also evident in the Leaf Area Index (LAI)
 334 of trees. LAI values drop from around 1 in the rainy season to approximately 0.6 on the
 335 peak of the dry season (Hoffmann et al., 2005).

336 The degree of foliation in LPJmL-VR-SPITFIRE is given by the phenology status,
 337 which is updated daily (ranging from 0 = no leaves to 1 = full leaf cover) and derived by
 338 multiplication of four limiting functions, namely a water-limiting (f_{water}), light-limiting

339 (f_{light}), cold-limiting (f_{cold}) and heat-limiting (f_{heat}) function (Schaphoff et al., 2018;
340 Forkel et al., 2014). The shape parameters of f_{water} were chosen to reflect a behaviour
341 intermediate between the evergreen and the raingreen PFT (Fig. S3), and thereby reflects
342 the general phenological behaviour of the Cerrado community as explained above; f_{heat} ,
343 f_{cold} and f_{light} were set to the same values as for TrBE.

344 *2.3.4 Fire dynamic and vegetation adaptation*

345 ~~Over 10.5~~ Approximately 6 million hectares burned in the Cerrado in 202~~43~~
346 (MapBiomas Fogo 202~~54~~43), with 98% of these fires attributed to human activity
347 (Schumacher et al., 2022). At local and landscape scales, fire dynamics are influenced by
348 factors such as fuel availability, ignition sources, topography, and climatic conditions
349 (Gomes, Miranda, and Bustamante 2018). In the Cerrado, fire behavior is closely tied to
350 seasonal cycles and one key factor determining its behavior is the vapor pressure deficit
351 (VPD) (Gomes, et al., 2020b; Oliveira et al., 2021). VPD is the measure of the difference
352 between the vapour pressure of the moisture present in the air and the maximum vapour
353 pressure the air can hold, being influenced by temperature and relative humidity. In the
354 Cerrado, the VPD varies seasonally, with average values around 0.3 to 0.7 kPa in the rainy
355 season and 1.4 to 2.0 kPa in the dry season (Cattelan et al., 2024). Higher VPD dehydrates
356 plant biomass, especially from grasses, making it more flammable and susceptible to fire
357 (Gomes, et al., 2020b). The VPD affects the rate of spread and intensity of the fire, with
358 higher VPD resulting in faster and more intense fires in a given fuel bed (Gomes et al.,
359 2020b; Oliveira et al., 2021). In LPJmL-VR-SPITFIRE, the fire danger index depends on
360 VPD and is scaled via a PFT-specific factor α VPD, where higher values of α VPD increase
361 fire danger. We calibrated α VPD to achieve good agreement between observed and
362 modelled burnt area. A higher α VPD for TrBS than for TrBE and TrBR was chosen,

363 because the fuel produced by the Cerrado trees burns more readily, compared to the fuel
364 dropped by trees in the moist forests (dos Santos et al., 2018).

365 Because of its fire-prone environment, the Cerrado trees exhibit several adaptations that
366 enable them to survive fire damage. These include belowground organs that promote
367 resprouting after fire, thick bark that insulates and protects internal tissues, robust terminal
368 branches, leaves concentrated at branch tips, and persistent stipules that safeguard apical
369 buds, all minimize fire damage (Simon et al., 2009; Simon and Pennington 2012). Fire-
370 induced tree mortality in LPJmL-VR-SPITFIRE results from combined effects of cambial
371 and crown damage (Oberhagemann et al., 2025). PFT-specific parameters for bark
372 thickness were chosen to fit the relationship between stem diameter and bark thickness
373 shown in Hofmann et al., (2009) (Fig. S3; Table 2). Scorch height, the highest point at
374 which flames reach and affect the vegetation, is calculated from fire intensity and a PFT
375 specific scaling factor (F ; see Eqn. S5), which also depends on tree crown length relative
376 to its height (Thonicke et al., 2010; Oberhagemann et al., 2025). The Cerrado trees have
377 relatively long crowns compared to their total height, with a ratio of 0.53 (Table 2). While
378 this exposes them to crown scorch, the above-mentioned adaptations result in an overall
379 lower mortality risk from crown scorch, and we therefore adjusted the parameter F
380 accordingly (Table 2).

381
382
383
384 Table 2: Fire parameters used to define the new Tropical Broadleaved Savanna Tree
385 (TrBS) PFT, along with the corresponding values for the Tropical Broadleaved Evergreen
386 Tree (TrBE) and Tropical Broadleaved Raingreen Tree (TrBR) PFTs. References cited

387 apply exclusively to TrBS PFT. SPITFIRE parameters for TrBE and TrBR are taken from
 388 (1) Thonicke et al., (2010), and (2) Drücke et al., (2019).

Parameter	Tropical Broadleaved Evergreen tree	Tropical Broadleaved Raingreen tree	Tropical Broadleaved Savanna tree	Reference
Leaf Longevity (years)	1.6	0.5	1	Cianciaruso et al., (2013); Souza, J. P. (2012)
Sensitivity to drought (c_{sens})	100	100	10	
Water stress resistance (c_{res})	0.1	0.1	0.1	
Water limitation factor ($wscal_{min}$)	0	0.35	0	
α VPD	6	6	10	
Crown length parameter	0.3334 ₍₁₎	0.10 ₍₁₎	0.53	Field survey (Table S2)
Scorch height parameter (F)	0.193 ₍₂₎	0.0799 ₍₂₎	0.13	
Bark thickness par1/par2	0.0301/0.0281 ₍₁₎	0.1085/0.212 ₍₁₎	0.135/0.2820	Hoffmann et al., (2009)

389

390 **2.4 Simulation protocol**

391 To evaluate the performance of the newly implemented TrBS PFT, two simulation runs
 392 were conducted: one including TrBS PFT (hereafter ‘Savanna’ simulation) and the other

393 experiment excluding it (hereafter ‘No Savanna’ simulation). Both simulations covered
394 the period from 1901 to 2019, with a 5000-year spin-up phase, and utilized identical
395 environmental input data in a 0.5° horizontal resolution.

396 The model spin-up was simulated from bare ground using climate input from 1901-
397 1930 (with pre-industrial $p\text{CO}_2 = 276.59$ ppm), which was repeated for 5000 years, to
398 allow carbon pools to reach equilibrium with climate. The transient simulation then ran
399 from 1901 to 2019. For model validation, we analyzed the last 30 years of the transient
400 run. Because we aim to evaluate the establishment and general characteristics of the new
401 TrBS PFT, all simulations were conducted for potential natural vegetation (PNV) only,
402 with no simulation of human land use to focus on geographical distribution of vegetation
403 and fire. While LPJmL-VR-SPITFIRE features the latest model updates regarding the
404 nitrogen cycle (Bloh et al., 2018) and biological nitrogen fixation (Wirth et al., 2024), we
405 switched the nitrogen limitation off as it was beyond the scope for this study.

406 The LPJmL-VR-SPITFIRE model uses daily climate input, including air temperature,
407 precipitation, wind speed, humidity, and long- and shortwave radiation. These datasets
408 were sourced from ISIMIP3a (<https://data.isimip.org/10.48364/ISIMIP.664235.2>), which
409 combines GSWP3 data (1901–1978) and W5E5 data (1979–2019). Atmospheric CO_2
410 concentration data were derived from the TRENDY project (Friedlingstein et al., 2023).

411 Soil texture data were obtained from the Harmonized World Soil Database
412 (Nachtergaele et al., 2009). Soil depth in LPJmL-VR-SPITFIRE was defined using the
413 lower water table depth values provided by the SOIL-WATERGRIDS dataset (Guglielmo
414 et al., 2021).

415 Ignition sources for the SPITFIRE model are based on population density (Klein
416 Goldewijk et al., 2011) for human ignitions, and lightning occurrence data from the
417 OTL/LIS dataset (Christian et al., 2003) for natural ignitions.

418

419 **2.5 Model validation**

420 For each of our simulation outputs, we selected appropriate Brazilian or global datasets
421 to validate the modeled results from LPJmL-VR-SPITFIRE. All spatial analysis and
422 comparisons between the validation data and model outputs were conducted in R, utilizing
423 the ncdf4, terra, raster and sf packages. The analysis focused on the mean values of the last
424 30 years of the simulations (1990-2019). Details of each validation dataset are provided
425 below.

426 *2.5.1 Vegetation distribution*

427 To validate the modeled distribution of the vegetation in Brazil, represented by the
428 foliar projected coverage (FPC) of each PFT, we used Brazil's original vegetation
429 distribution by IBGE (2017). The original IBGE map was a very detailed Shapefile, with
430 specific variation of each major vegetation group, that would have complicated the
431 comparison with the FPC and limited number of PFTs. For this reason, we aggregated the
432 vegetation classes into 13 vegetation types following the attribute table of IBGE's product
433 (Fig. 4). After that, we converted the Shapefile into a raster file using the function rasterize
434 from the terra package in R.

435 To evaluate the distribution of the new TrBS PFT, as well as the other tropical PFTs,
436 we overlaid the FPC output with the corresponding classification from IBGE. For this
437 comparison, we selected only grid cells where the respective $FPC \geq 0.3$ and matched the
438 class in the IBGE dataset, generating a map that identifies under-, over-, and correctly
439 simulated PFT coverage.

440 *2.5.2 Above- and belowground Biomass, evapotranspiration and productivity*

441 The above- and belowground biomass (AGB and BGB) validation maps were produced
442 by the team from the Fourth National Communication to the United Nations Convention
443 of Climate Change, here referred to as QCN (MCTI 2020). These maps were produced
444 considering the distribution of Brazil's original vegetation (IBGE 2017) and estimating
445 AGB and BGB using specific equations and field data that best fit each vegetation type.
446 From these maps we derived a BGB:AGB ratio map to validate the structural
447 characteristics of TrBS PFT. For better comparison, we calculated the Spearman
448 Correlation between the two modeled scenarios of BGB:AGB and the QCN validation
449 using the stats package from R software.

450 For evapotranspiration (ET) and gross primary productivity (GPP), the mean annual
451 distribution of the last 30 simulation years (1990-2019) were compared to reference
452 datasets (GPP: Carvalhais et al., 2014; ET: ERA~~5-Interim-Land~~, HersbachBalsamo et al.,
453 ~~2015~~2020) and evaluated via the Normalized Mean Squared Error (NMSE) and Pearson
454 correlation (as described in Sakschewski et al., 2021).

455 *2.5.3 Burned Area*

456 The Burned Area validation map was produced using the annual burned coverage
457 product from MapBiomas Fogo 3.0 (202~~43~~) database. This product gives a 30 m resolution
458 presence-absence map of areas in which fire occurred for a time series from 1985 to 2023.
459 The burned area was calculated from the burned coverage for a 0.5° grid, covering all the
460 Brazilian territory, for each year from 1990 to 201~~98~~98. Then, from resulting annual burned
461 area maps, we calculated the mean burned area for all selected time series. All calculations

462 and map generation from the MapBiomas dataset were performed using the Google Earth
463 Engine platform.

464 For the spatial distribution of annual burned area, we created a map of the human land-
465 use fraction based on MapBiomas 9.0 land-use data (MapBiomas, 202⁴³), using the mean
466 value from 1990 to 2019 (Fig. S5). Since our simulation considers only potential natural
467 vegetation (PNV), we weighted the burned area, in both the validation data and model
468 output, to account for fire occurrences in human-managed land.

469 The validation of the monthly burned area for the Cerrado biome was conducted using
470 the MapBiomas Fogo 3.0 dataset (202⁴³). The burned area validation was also weighted
471 by the natural land-cover of the corresponding year. This dataset was used to assess the
472 accuracy of the simulated seasonal burned area patterns in the Cerrado. The comparison
473 between the simulated scenarios and the MapBiomas data was evaluated using Normalized
474 Mean Squared Error (NMSE), Willmott's index, R^2 , and p-value statistics from the
475 respective R packages kerntools, hydroGOF and stats (Drücke et al., 2019).

476 For carbon emission by fire (FireC), our validation is based on the Global Fire
477 Emissions Database (GFED4), which derives its fireC emission maps using its own burned
478 area data (van der Werf et al., 2017). GFED4 combines satellite observations of burned
479 area with biogeochemical modeling to estimate emissions of CO₂, CO, CH₄, and other
480 trace gases. Given the strong link between burned area and fire emissions, we apply the
481 same land-use fraction weighting approach as for burned area to ensure consistency in our
482 analysis.

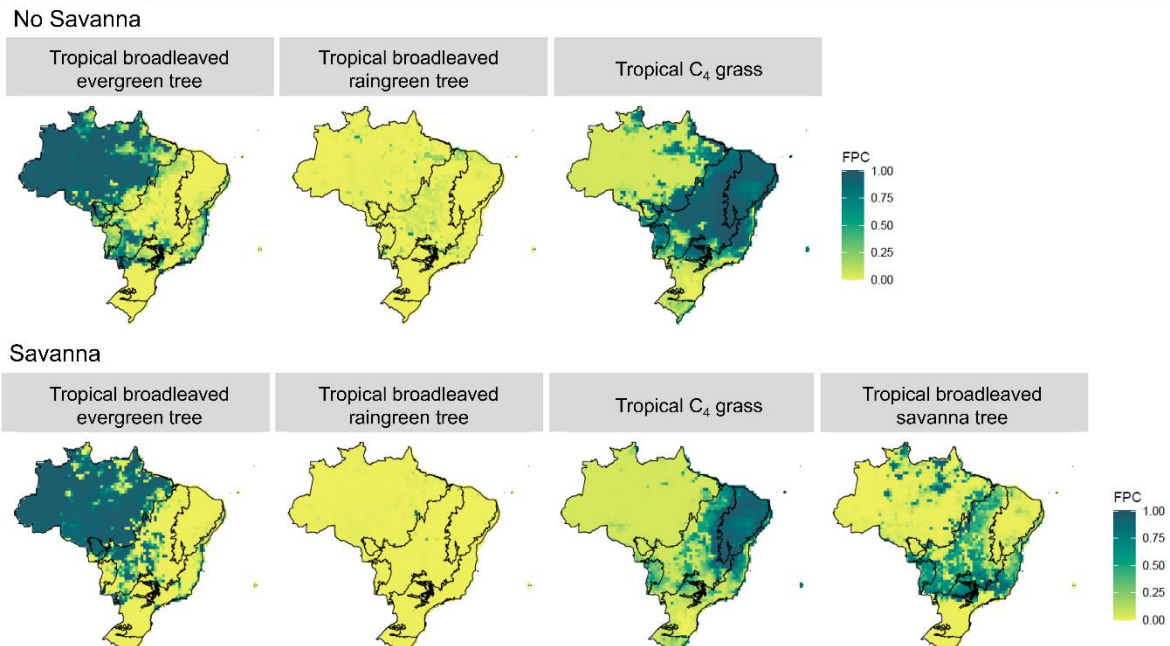
483 **3. Results**

484 ***3.1 Vegetation distribution***

485 The inclusion of TrBS PFT [and the implementation of the Drought Mortality](#)
486 [Function haveas](#) significantly altered the distribution and abundance of key vegetation
487 types across Brazil, particularly the Tropical C₄ grasses and TrBE PFTs [\(see the](#)
488 [supplementary file for further information](#)[\).](#) In simulations without TrBS, C₄ grass
489 dominates across northeastern and central Brazil, occupying the whole Caatinga biome,
490 most of the Cerrado and northern Atlantic Forest (Fig. 3).

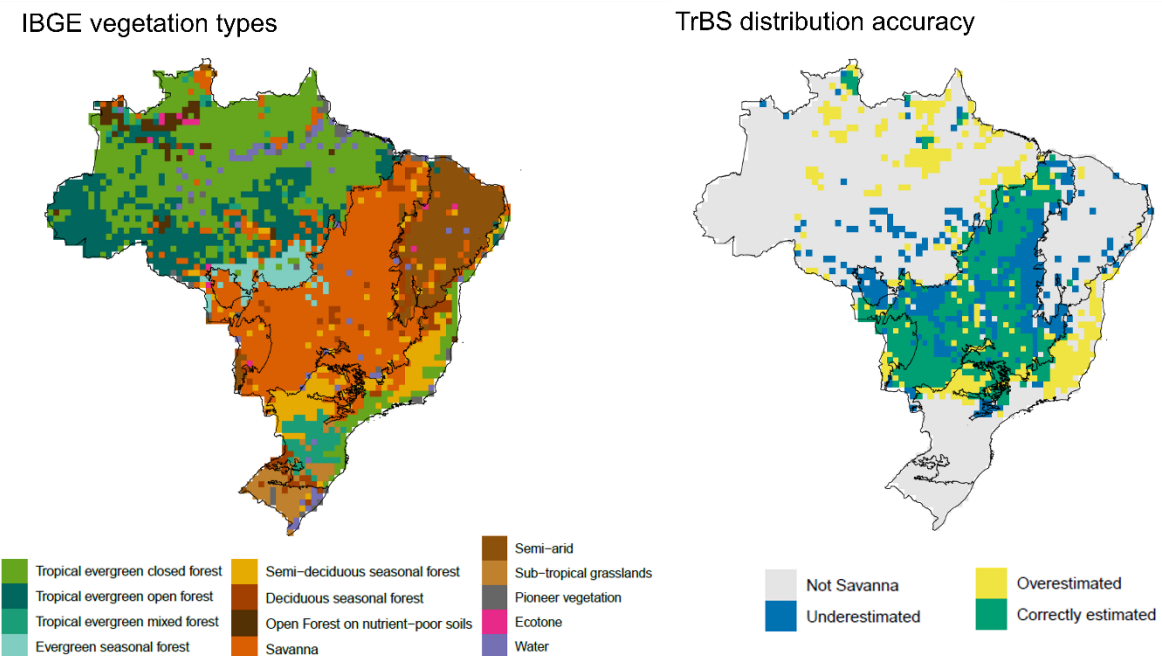
491 TrBS establishes itself predominantly in the Cerrado and Pantanal biomes, aligning
492 with regions classified as savanna vegetation by IBGE (Figs. 3 and 4). Pockets of TrBS
493 also appear in northern portions of the Amazon biome, where patches of savanna-like
494 vegetation can occur, and Atlantic Forest regions where seasonal forest is present (Fig.
495 3 and 4). The presence of TrBS results in a contraction of C₄ grass, which retreats mostly
496 to the Caatinga biome, where they almost entirely dominate due to Caatinga's dry
497 environment, while grass and savanna vegetation coexist in Pantanal, northern and
498 eastern Cerrado (Fig. 3).

499



500
501
502
503
504
505

Fig. 3: Foliar Projected Cover (FPC) of the Plant Functional Types (PFT) for Tropical Broadleaved Evergreen Tree, Tropical Broadleaved Raingreen Tree, Tropical C₄ Grass and Tropical Broadleaved Savanna Tree in Brazil under two model configurations: 'No Savanna' and 'Savanna'.



506

507 Fig. 4: Maps showing the Brazilian vegetation types according to IBGE (left) and TrBS
508 PFT distribution accuracy (right) in comparison with the savanna vegetation class from
509 IBGE. A threshold of 30% FPC cover was used to determine distribution accuracy.

510

511 **3.2 Above- and belowground Biomass and vegetation structure**

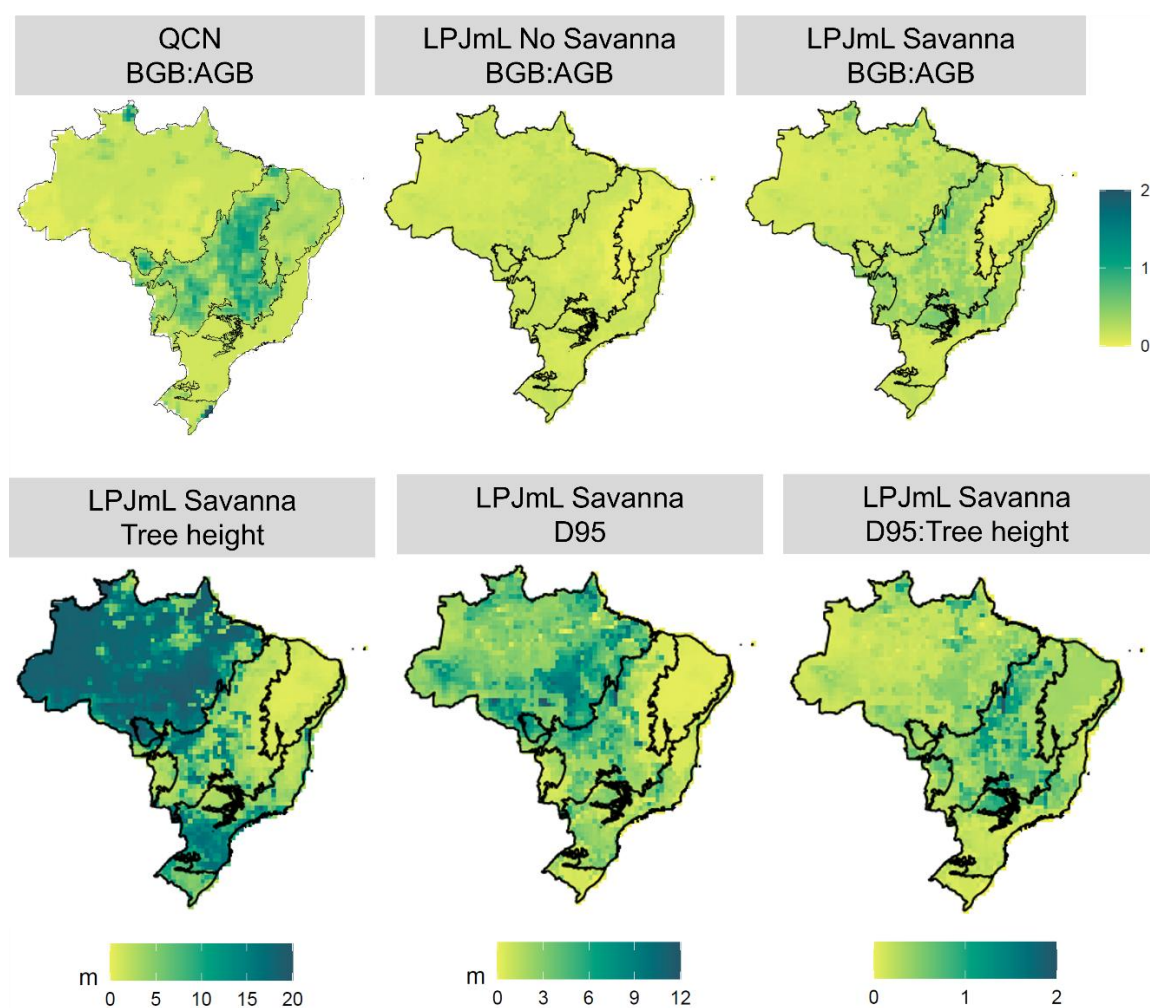
512 The inclusion of TrBS PFT significantly improved the simulated above- and
513 belowground biomass patterns across Brazil compared to simulations without it. By better
514 capturing the characteristic small trees with extensive belowground structures of the
515 Cerrado, TrBS PFT led to an improved representation of the 'upside-down forest' in central
516 Brazil (Fig. 5). As a reflection of the distinct allocation strategies of the Cerrado
517 vegetation, the biomass ratio (BGB:AGB) was also clearly improved in the Savanna
518 scenario (Fig. 5). Although the simulated values did not fully match those observed in the
519 QCN validation, as shown by the Spearman correlations (QCN vs. Savanna: 0.27; QCN
520 vs. No Savanna: -0.16), the introduction of TrBS resulted in a more accurate simulation of
521 carbon allocation across Brazil. Both scenarios also showed good performance relative to
522 the reference data for GPP (NMSE < 1), with the Savanna model having a marginally lower
523 error compared to the No Savanna (Fig. S10; Table S3). For ET, deviations from the
524 validation dataset are large for both scenarios, with the No Savanna having a slightly better
525 performance (NMSE = 1.56) compared to the Savanna (NMSE = 1.89) (Fig. S10; Table
526 S3).

527 ~~Normalized Mean Error (NME) and correlation of modelled ET (and GPP across Brazil~~
528 ~~were in a similar range for both simulations in comparison to the reference data (Fig. S9;~~
529 ~~Table S3).~~

530 TrBS PFT also improved the representation of tree height gradients, with tall trees,
531 above 20 m, in the Amazon transitioning to slightly shorter trees in the southern Amazon

532 and reaching approximately 7 m in the Cerrado (Fig. 5; Fig. S7). Additionally, the model
533 now captures a gradient in rooting depth (D95), with shallower roots in the Amazon,
534 deepening towards the southern Amazon and Cerrado (Fig. 5; Fig. S7). This pattern is
535 further supported by a higher D95:height ratio in the Cerrado, aligning with the
536 characterization of its vegetation as an 'upside-down forest,' where rooting depth can
537 exceed tree height.

538



539

540 Fig. 5: FPC-weighted BGB:AGB below- and aboveground biomass ratio (BGB:AGB)
541 from LPJmL simulations and QCN validation product (top row), and FPC-weighted tree
542 height and D95, and their ratio (D95:Tree height) from LPJmL 'Savanna' simulation
543 (bottom row).

544

545 **3.3 Fire dynamics**

546 The introduction of TrBS PFT significantly influenced burned area patterns across
 547 biomes. LPJmL-VR-SPITFIRE generally underestimated burned areas in the ‘No
 548 Savanna’ simulation, particularly in the Cerrado and Amazon regions, while
 549 overestimating them in the Caatinga (Table 3; Fig. 6). With the inclusion of the new TrBS
 550 PFT, the burned area estimates in the Cerrado increased, surpassing the values recorded in
 551 the MapBiomas Fogo in ~~the~~ central Cerrado, but still underestimating burned area in the
 552 northern region of Cerrado and in the Amazon (Fig. 6). ~~In contrast, the Amazon continued~~
 553 ~~to show underestimations of burned areas, likely due to the general assumption of higher~~
 554 ~~human-caused ignitions in rural areas not capturing the real motivations to set fire.~~ Despite
 555 these regional discrepancies and given the SPITFIRE improvements applied to both model
 556 configurations, the inclusion of TrBS PFT and its adjusted parameterizations led to a clear
 557 improvement in the total burned area estimates for Brazil (Table 3).

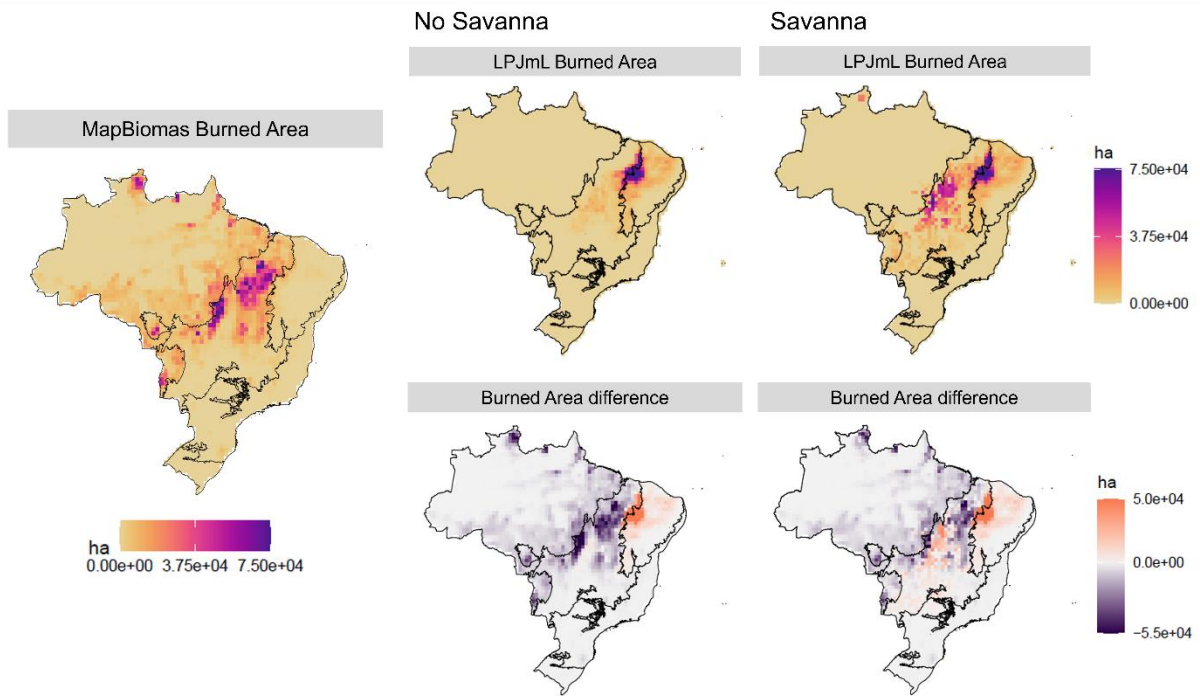
558

559 Table 3: Total burned area for all Brazilian biomes simulated by LPJmL-VR-SPITFIRE
 560 for ‘Savanna’, and ‘No Savanna’ scenarios, and the validation data from MapBiomas
 561 Fogo. The values are in Thousand hectares (Kha).

	Savanna (Kha)	No Savanna (Kha)	MapBiomas (Kha)
Cerrado	6660.7	2597.21	7748.43
Amazon	405.67	44.48	4991.57
Atlantic Forest	89.69	5.82	130.83
Caatinga	2937.68	2818.43	345.6
Pantanal	203.84	5.33	558.55
Pampa	1.15	1.15	11.89
Brazil	10298.73	5472.42	13786.89

562

563



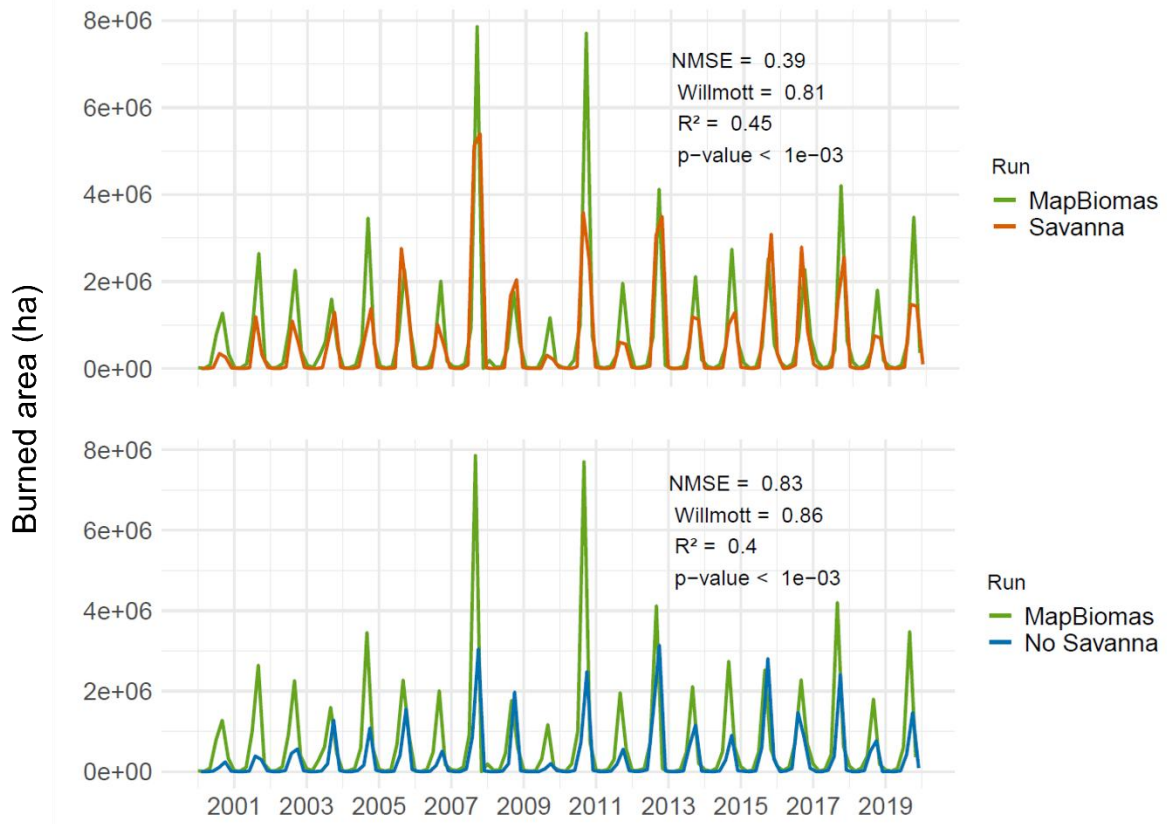
564

565 Fig. 6: LPJmL simulations of burned area in Brazil for ‘No Savanna’
 566 scenarios (top row), the validation data by MapBiomas Fogo (left), and the respective
 567 difference between simulated results and MapBiomas Fogo validation (bottom row).

568

569 We could also observe an improvement in the seasonal patterns of the burned area in
 570 the Cerrado Biome with the incorporation of TrBS PFT (Fig. 7). The Savanna scenario,
 571 compared to the MapBiomas data, shows an NMSE of 0.39 with an R^2 of 0.45, and a
 572 Willmott index of 0.81, indicating that the model has a good fit. The No Savanna scenario
 573 has a slightly higher NMSE (0.83) and Willmott index (0.86), and a lower R^2 (0.40)
 574 compared to MapBiomas, suggesting that removing TrBS reduces the overall model’s
 575 ability to represent observed seasonal fire patterns.

576



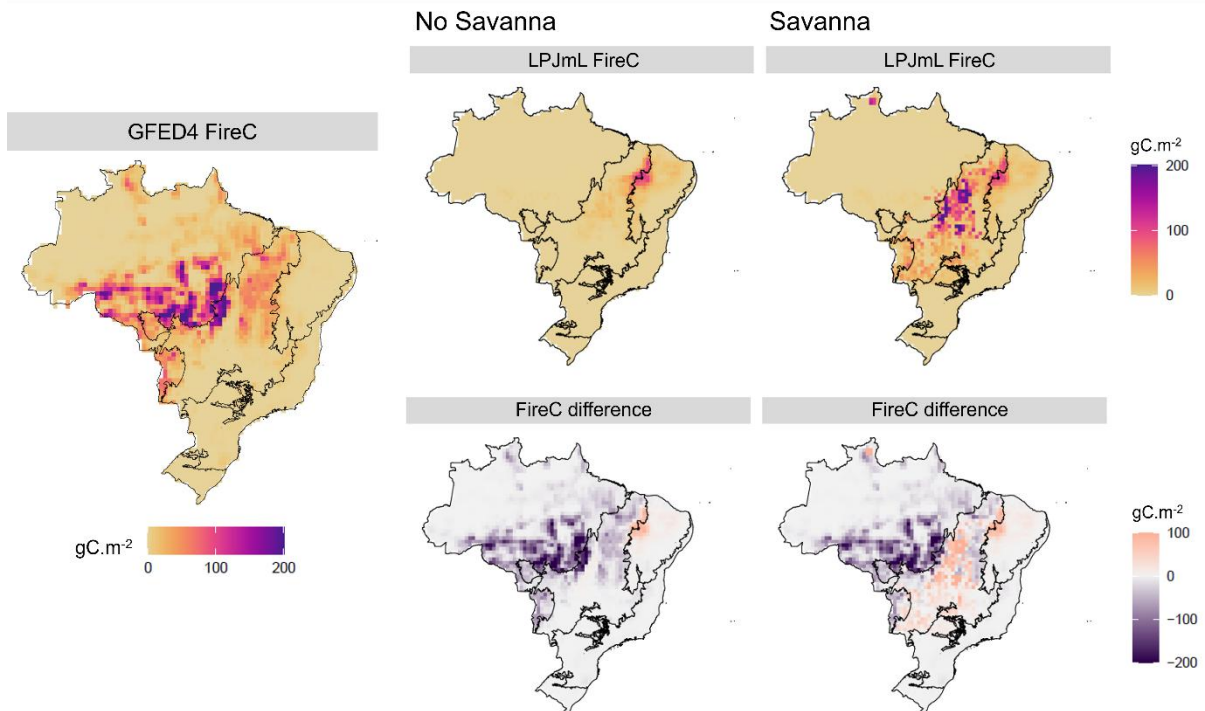
577

578 Fig. 7: Total monthly burned area, for the Cerrado Biome, from 2000 to 2019 for two
 579 LPJmL simulation scenarios: 'Savanna' (top) and 'No Savanna' (bottom) in comparison
 580 with the monthly burned area product from MapBiomas Fogo.

581

582 Carbon emission by fire (FireC) patterns reflect directly the burned area patterns (Fig.
 583 8). Overall, the introduction of TrBS did not improve emission estimates in Brazil as most
 584 of the emission comes from southeastern Amazon, which has its burned area highly
 585 underestimated by our model. ~~In the Cerrado, fire-related emissions were overestimated in~~
 586 ~~the Savanna scenario, particularly in the central part of the biome, reflecting the spatial~~
 587 ~~patterns of burned area. Fire-related emissions in the Cerrado, on the other hand, were~~
 588 ~~overestimated in the Savanna scenario, especially in the central portion of the biome,~~
 589 ~~which is linked to the spatial burned area patterns.~~

590



591

592 Fig. 8: LPJmL simulations of Fire carbon emission in Brazil for No Savanna
 593 scenarios (top row), the validation data by GFED4 (left), and the respective difference
 594 between simulated results and GFED4 validation (bottom row).

595

596 ***3.4 Extrapolation to the global scale***

597 Since the LPJmL-VR-SPITFIRE model will also be run on a global scale in future
 598 applications, the parameterization of the new PFT was tested in a global simulation using
 599 the same climate input data set as for the Brazilian simulations. Although TrBS PFT was
 600 specifically adapted to the Cerrado tree data, we found high agreement in the simulated
 601 global savanna distribution compared to a reference dataset (Hengl et al., 2018). The
 602 results are shown in Supplementary Fig. S⁹⁸.

603

604 **4. Discussion**

605 ***4.1 Advancing in Savanna Modeling***

606 The introduction of a savanna-specific Plant Functional Type in the LPJmL-VR-
607 SPITFIRE model significantly enhances the representation of vegetation and fire dynamics
608 in Brazil. TrBS improved simulations of carbon allocation, particularly below- to
609 aboveground biomass ratio, and better represented fire behavior, especially the, namely
610 ~~the spatial distribution and~~ temporal dynamics of burned area. Key features of the Cerrado,
611 that also apply to tropical savannas in general, are now well represented: a vegetation that
612 is adapted to seasonal drought environments by accessing water with deep root systems
613 and allocating more resources belowground and can cope with or even depends on regular
614 occurring fires. This update moves the capability of LPJmL-VR-SPITFIRE beyond the
615 previous binary classification of tropical rainforests and grasslands, allowing for a more
616 nuanced depiction of ecological transitions, such as the Amazon-Cerrado interface. By
617 incorporating savanna vegetation, the model facilitates more realistic investigations into
618 the future dynamics of these biomes and allows for a more critical evaluation of restoration
619 efforts within this specific vegetation type. A model limited to representing only 'forest'
620 and 'grasslands' will fail to capture the significance and vulnerabilities inherent in savanna
621 ecosystems like the Cerrado.

622 Other DGVMs have struggled earlier to accurately depict the savanna biome (Whitley
623 et al., 2017; Baudena et al., 2015), as many of them oversimplify root dynamics, specific
624 phenology and vegetation-fire feedback. In particular, the role of rooting depth, which is
625 often constrained to shallow values in DGVMs, has a significant impact on the competition
626 between forest, savanna vegetation and grasses, as shown by Langan et al., (2017) for
627 South America. The introduction of root growth and rooting depth diversity in the LPJmL
628 model (Sakschewski et al., 2021) can therefore be considered key to improving savanna

629 modeling, as it allows vegetation adaptation to water scarcity, especially when subdividing
630 the PFTs into different rooting strategies. Importantly, the competition for water between
631 savanna trees and grasses can also be better depicted when partitioning of access to water
632 resources is considered (Whitley et al., 2017; Baudena et al., 2015).

633 ~~The SPITFIRE model provided a process-based calculation of ignition, fire spread and~~
634 ~~tree fire mortality that is central to better reproduce typical Cerrado and savanna biome~~
635 ~~characteristics. However, the often extensive use of fire for land management purposes in~~
636 ~~savannas (and, for example, also the edges of Amazonia) is not explicitly reflected in~~
637 ~~SPITFIRE, as the model only considers a function of population density to calculate~~
638 ~~ignition risks. Recent attempts to better reflect anthropogenic fire management (Perkins et~~
639 ~~al., 2024) could help further improve Cerrado fire modeling. Given the increasing pressure~~
640 ~~on the Cerrado and already observed shifts in fire regimes (da Silva Arruda et al., 2024),~~
641 ~~this is key to enabling simulations of future trajectories in the region. While accurate fire-~~
642 ~~vegetation dynamics are crucial for realistic biome distribution simulations, they are~~
643 ~~insufficient if key vegetation characteristics, such as deep root water uptake, are not~~
644 ~~adequately represented (D'Onofrio et al., 2020, Baudena et al., 2015).~~

645 We parameterized the savanna tree PFT using field and literature data specific to the
646 Brazilian Cerrado region and achieved a good fit between modelled and observed savanna
647 distribution. Other modeling studies, for example Moncrieff et al., (2016), have
648 encountered challenges to capture the Cerrado extent due to missing processes.
649 Extrapolations of model parametrization that were specifically evaluated for one savanna
650 region, here the Cerrado, often leads to inaccuracies, given the distinct climate, species
651 composition, and fire-vegetation interactions in each of the savanna-type regions (Solbrig
652 et al., 1996; Lehmann et al., 2014; Moncrieff et al., 2016). Nevertheless, to assess the
653 robustness of our parameterization, we conducted a global simulation and found that the

654 parameterization developed for the Brazilian savanna performed well in simulating global
655 tropical savanna distributions (Fig. S97). Future work could also include an assessment to
656 better capture main functional differences between each savanna-type region.

657

658 ***4.2 Challenges in Representing the Cerrado Dynamics***

659 Despite these advancements, several challenges remain in capturing the complex
660 vegetation dynamics of the Cerrado. Although our simulations already produce a mix of
661 savanna trees and grasses in the northern Cerrado, one key issue is achieving a realistic
662 balance and dynamic feedback between tree and grass cover. Achieving a more realistic
663 vegetation structure is challenging with representing tree and shrub individuals as
664 generalized representatives of each PFT, even though differentiations by rooting depth
665 were incorporated in LPJmL-VR-SPITFIRE. Building on the knowledge gained in this
666 study a gap-model framework that simulates individual trees and also incorporates trait
667 diversity such as the LPJmL-FIT model (Sakschewski et al., 2015; Thonicke et al., 2020),
668 could offer a more accurate representation of tree-grass coexistence in the near future.

669 Our analysis focused on depicting the overall distribution and performance of the new
670 savanna PFT across Brazil. A detailed, site specific validation of carbon and water fluxes,
671 the seasonality of leaf cover and productivity might complement the results of this study.
672 In this context, further model refinement could be undertaken, such as implementing shade
673 intolerant PFTs in the model (Ronquim et al., 2003; Lemos-Filho et al., 2010).
674 Additionally, a notable limitation observed in our simulations is the overrepresentation of
675 C₄ grasses in the Caatinga biome, which contrasts with the known vegetation
676 characteristics of the region. The Caatinga is a semi-arid biome characterized by diverse
677 vegetation physiognomies, including succulents and small shrub vegetation, with a
678 predominance of seasonal dry tropical forests rather than extensive grasslands (de Queiroz

679 et al., 2017). ~~In follow up work with LPJmL-VR-SPITFIRE, it should be determined~~
680 ~~which PFT combination is closest to this complex real world vegetation.~~ As discussed for
681 the tree-grass coexistence in the previous paragraph, Caatinga vegetation modeling would
682 benefit from an individual tree approach (as in LPJmL-FIT) rather than the average
683 individual approach of the LPJmL model. Addressing this will be important for improving
684 model realism and its applicability to drier tropical ecosystems, as well as enhancing its
685 performance in representing fire patterns in the region.

686 Fire impacts on the vegetation are a key process that maintains savannas' open-canopy
687 structure. Our parameterization of the savanna tree PFT resulted in a vegetation type with
688 high flammability, yet is well protected against lethal fire damage that is readily burning,
689 while being well protected against lethal damage from fire. However, resprouting
690 mechanisms, which are crucial for post-fire recovery (Souchie et al. 2017) are not yet
691 implemented explicitly in the vegetation model but would improve the simulation of
692 vegetation recovery. The amount of fuel available for burning is another key area of
693 ongoing model development, as it strongly influences fire spread and intensity. In the most
694 recent SPITFIRE version that we used in this study, the live grass moisture calculation was
695 substantially improved (Oberhagemann et al., 2025), better reflecting seasonal dynamics
696 of fuel availability of grass vegetation. Although the inclusion of the TrBS PFT may
697 improve the representation of vegetation structure and total biomass in the Cerrado, we
698 could not assess whether this translated into an improvement in fuel biomass estimates. In
699 SPITFIRE, leaves and a proportion of sapwood and heartwood from twigs, branches, and
700 trunks are considered to calculate living fuel biomass (Thonicke et al., 2010). QCN
701 products, on the other hand, do not distinguish carbon stored in these specific tree
702 components but only report total above- and belowground biomass; therefore, a direct
703 validation or assessment of fuel biomass improvement resulting from the TrBS

704 ~~implementation was not feasible. However, currently live woody materials are not~~
705 ~~parametrized as part of the burnable matter in SPITFIRE, but this is potentially important~~
706 ~~in Cerrado (Oliveira et al., 2021).~~

707 In Savannas, there is often extensive use of fire for land management purposes.
708 Specifically, in the Cerrado, fire in natural areas is associated with the use of fire for
709 deforestation and pasture management, with fire escaping to natural areas, while in areas
710 of mechanized agriculture and planted forests, owners rather protect the areas against fire.
711 In SPITFIRE, however, ignitions are represented solely as a function of population density,
712 and the model does not explicitly capture the diverse fire management regimes common
713 in these regions. This simplification contributes to the underestimation of burned area
714 along the Caatinga border, where expanding deforestation and intensive land management
715 interact with natural fire regimes, as well as in southeastern Amazonia, where large-scale
716 pasture management fires may escape and affect adjacent rainforest (MapBiomas Fogo,
717 2024; Cano-Crespo et al., 2015). To mitigate this, we weighted both validation data and
718 model outputs by the human land-use fraction from MapBiomas, thereby excluding grid
719 cells with extensive anthropogenic land use from the analysis. Recent attempts to better
720 incorporate anthropogenic fire management into models (Perkins et al., 2024) could
721 enhance Cerrado fire simulations, which is particularly relevant given the increasing
722 pressures on the biome and the ongoing shifts in fire regimes (da Silva Arruda et al., 2024).
723 Nevertheless, even with improved fire-vegetation dynamics, simulations of future
724 trajectories of these dynamics will remain constrained if key vegetation traits, such as deep
725 root water uptake, are not adequately represented (D’Onofrio et al., 2020; Baudena et al.,
726 2015).

727 In Savannas, there is often extensive use of fire for land management purposes.
728 Specifically, in the Cerrado, fire in natural areas is associated with the use of fire for

729 ~~deforestation, with fire escaping to natural areas and also with pasture management; in~~
730 ~~areas of mechanized agriculture and planted forests, owners rather protect the areas against~~
731 ~~fire. The underestimation in burned area observed in southeastern Amazon is also a product~~
732 ~~of such land-use change practices, especially the usage of fire to manage large extension~~
733 ~~of pasturelands in Amazon (MapBiomas Fogo, 2024) which could possibly escape and~~
734 ~~damage adjacent tropical rainforest (Cano-Crespo et al., 2015). The SPITFIRE model does~~
735 ~~not explicitly account for different fire management regimes but scales ignitions to human~~
736 ~~population density. This might explain the lack of fire at the edges of Amazonia in our~~
737 ~~simulations and also complicates validation of burned area and fire carbon emissions from~~
738 ~~our PNV simulations. We therefore weighted both validation data and model output by the~~
739 ~~human landuse fraction from MapBiomas to exclude grid cells with extensive human land~~
740 ~~use from the analysis.~~

741 The most recent version of LPJmL incorporates the nitrogen cycle (von Bloh et al.,
742 2018), along with mechanisms of biological nitrogen fixation (BNF, Wirth et al., 2024).
743 Soils in the Cerrado are characterized by acidity, high aluminum concentrations, and
744 nutrient scarcity (Bustamante et al., 2006; 2012), requiring vegetation to develop specific
745 adaptations that confer a competitive advantage in these nutrient-poor conditions. Future
746 advancements should leverage these model enhancements to incorporate nitrogen and
747 other nutrient constraints, enhancing ecological realism to specifically address this aspect
748 to the complex ecological interactions.

749 Beyond the factors already discussed, rootable soil depth significantly influences
750 vegetation dynamics. However, determining the maximum depth roots can physically
751 penetrate is challenging, as they can grow into bedrock and access groundwater, but are
752 also limited by high soil density and low oxygen availability. In our simulations we used
753 the water table depth of Guiglemo et al., (2021) as a proxy for rootable soil depth, which

754 allows deep rooting over large parts of the Cerrado, in line with observations of deep
755 rooting vegetation. While this method provides reasonably spatial variable maximum
756 rooting depths, LPJmL-VR-SPITFIRE does not simulate an actual water table. In reality,
757 deep-rooted trees can tap groundwater, but LPJmL-VR-SPITFIRE assumes free drainage,
758 preventing this interaction. Consequently, some areas may experience artificially shallow
759 rooting depths (e.g. Amazonian floodplains) without the benefit of accessing deeper water
760 reserves, a factor that could become important, especially when running future simulations
761 with the model. Considering these aspects in future work, especially global studies, could
762 further improve the representation of belowground competition and resulting spatial
763 vegetation distribution.

764 5. Conclusion

765 The parameterization of the new Tropical Broadleaved Savanna PFT (TrBS) in LPJmL-
766 VR-SPITFIRE significantly improves the representation of the Cerrado biome, the second-
767 largest vegetation formation in South America, in terms of belowground vs aboveground
768 competition, vegetation dynamics and fire. By inclusion of variable rooting strategies
769 along with recent process-based fire modeling, and a new drought mortality function, we
770 present a model that is suited to study complex ecological interactions of the sensitive
771 Cerrado biome that are rapidly changing under ongoing climate change. Here, we
772 combined literature and observational data to parameterize the TrBS PFT and to adjust
773 parameters of tree and root allocation functions, among others. Introducing a dedicated
774 vegetation type for tropical savannas and combining with variable rooting strategies will
775 equip DGVMs to make more precise assessments of recovery, reforestation, and
776 regeneration strategies in these unique ecosystems. By refining the modeling of savanna
777 dynamics, this study provides a valuable foundation for improving conservation strategies,

779 land-use planning, and climate mitigation efforts in fire-prone landscapes such as the
780 Cerrado. The introduction of a savanna-specific PFT with deeper rooting depth not only
781 led to a more realistic allocation of carbon belowground but also enabled the model to
782 reproduce the iconic “upside-down forest” structure of the Cerrado. This structural realism
783 also translated into better representation of vegetation distribution, fire regimes, and their
784 seasonal patterns. These results underscore the importance of incorporating trait diversity,
785 particularly rooting strategies, into DGVMs. Building on this progress, future work, such
786 as extending this savanna-specific PFT to individual-based models like LPJmL-FIT, can
787 further enhance our understanding of post-fire recovery dynamics interacting with
788 functional diversity and more clearly distinguish the intrinsic ecological behavior of
789 tropical savannas from that of tropical forests.

791 **6. Code and Data Availability**

792 The LPJmL-VR-SPITFIRE model is open-source and available at
793 [\[10.5281/zenodo.16965740](https://doi.org/10.5281/zenodo.16965740)*link will be added in future*]. Field survey data used in this
794 study are available from the corresponding author upon reasonable request. All other
795 relevant data supporting the findings of this study are available from the authors or
796 included in the supplementary materials.

798 **7. Competing interests**

799 One author is a member of the editorial board of journal "Biogeosciences".

801 **8. Author contributions**

802 *J.S.: Data curation, Formal analysis, Visualization, Writing – original draft

803 *S.B.: Methodology and Software, Formal analysis, Visualization, Writing – original

804 draft
805 W.v.B.: Methodology and Software, Writing – review and editing
806 M.Bi.: Methodology and Software, Writing – review and editing
807 B.S.: Conceptualization, Writing – review and editing
808 L.O.: Writing – review and editing
809 K.Th.: Supervision, Writing – review and editing
810 M.Bu.: Supervision, Writing – review and editing
811

812 **9. Acknowledgments**

813 The authors are grateful to PIK and the Graduate Program in Ecology from UnB for
814 providing the infrastructure and assistance without which this project wouldn't be possible.
815 To all researchers from the Ecosystems in Transition group at PIK and the Ecosystems
816 Ecology Lab at UnB that contributed with suggestions, critiques, points and ideas. Special
817 thanks to Letícia Gomes, Isabel Castro, Waira Machida, Lucas Costa and Felipe Lenti for
818 sharing their field data, essential for this work. Boris Sakschewski is part of the Planetary
819 Boundaries Science Lab.

820 821 **10. Funding Information**

822 J.S. acknowledges the funding by the National Coordination for High Level Education and
823 Training (CAPES) through the Internationalization Program (PrInt), grant number
824 88887.891863/2023-00. This work was supported by the National Institute of Science and
825 Technology for Climate Change Phase 2 under CNPq grant 465501/2014-1, FAPESP grant
826 2014/50848-9 and CAPES grant 88881.146050/2017-01. S.B. gratefully acknowledges
827 funding by the Conservation International Foundation, grant number CI-114129. This
828 project has received funding from the European Union's Horizon 2020 research and

829 innovation program under grant agreement No 101003890 (FirEURisk). The authors
830 gratefully acknowledge the Ministry of Research, Science and Culture (MWFK) of Land
831 Brandenburg for supporting this project by providing resources on the high-performance
832 computer system at the Potsdam Institute for Climate Impact Research.

833

834 **11. References**

835 ~~Balsamo, G., Albergel, C., Beljaars, A., Boussetta, S., Brun, E., Cloke, H., Dee, D., Dutra,~~
836 ~~E., Muñoz-Sabater, J., Pappenberger, F., de Rosnay, P., Stockdale, T., and Vitart, F.:~~
837 ~~ERA-Interim/Land: A global land surface reanalysis data set, Hydrol. Earth. Syst. Sc.,~~
838 ~~19, 389–407, <https://doi.org/10.5194/hess-19-389-2015>, 2015.~~

839 Baudena, M., Dekker, S. C., Van Bodegom, P. M., Cuesta, B., Higgins, S. I., Lehsten, V.,
840 Reick, C. H., Rietkerk, M., Scheiter, S., Yin, Z., Zavala, M. A., and Brovkin, V.: Forests,
841 savannas, and grasslands: Bridging the knowledge gap between ecology and Dynamic
842 Global Vegetation Models, Biogeosciences, 12, 1833–1848, <https://doi.org/10.5194/bg-12-1833-2015>, 2015.

844 Bowman, D. M. J. S., Balch, J. K., Artaxo, P., Bond, W. J., Carlson, J. M., Cochrane, M.
845 A., D'Antonio, C. M., DeFries, R. S., Doyle, J. C., Harrison, S. P., Johnston, F. H.,
846 Keeley, J. E., Krawchuk, M. A., Kull, C. A., Marston, J. B., Moritz, M. A., Prentice, I.
847 C., Roos, C. I., Scott, A. C., ... Pyne, S. J.: Fire in the Earth System, Science, 324, 481–
848 484, <https://doi.org/10.1126/science.1163886>, 2009.

849 Bustamante, M. M. C., Nardoto, G. B., Pinto, A. S., Resende, J. C. F., Takahashi, F. S. C.,
850 and Vieira, L. C. G.: Potential impacts of climate change on biogeochemical functioning
851 of Cerrado ecosystems. Braz. J. Biol., 72, 655–671, <https://doi.org/10.1590/S1519-69842012000400005>, 2012.

853 Bustamante, M. M. C., Silva, J. S., Scariot, A., Sampaio, A. B., Mascia, D. L., Garcia, E.,
854 Sano, E., Fernandes, G. W., Durigan, G., Roitman, I., Figueiredo, I., Rodrigues, R. R.,
855 Pillar, V. D., de Oliveira, A. O., Malhado, A. C., Alencar, A., Vendramini, A., Padovezi,
856 A., Carrascosa, H., ... Nobre, C.: Ecological restoration as a strategy for mitigating and

857 adapting to climate change: Lessons and challenges from Brazil. *Mitig. Adapt. Strat. Gl.*,
858 24, 1249–1270, <https://doi.org/10.1007/s11027-018-9837-5>, 2019.

859 Bustamante, M., Medina, E., Asner, G., Nardoto, G., and Garcia-Montiel, D.: Nitrogen
860 cycling in tropical and temperate savannas, *Biogeochemistry*, 79, 209–237,
861 <https://doi.org/10.1007/s10533-006-9006-x>, 2006.

862 Cano-Crespo, A., Oliveira, P. J. C., Boit, A., Cardoso, M., and Thonicke, K.: Forest edge
863 burning in the Brazilian Amazon promoted by escaping fires from managed pastures, *J.
864 Geophys. Res-Bioge.*, 120, 2095-2107, <https://doi.org/10.1002/2015JG002914>, 2015.

865 Carvalhais, N., Forkel, M., Khomik, M., Bellarby, J., Jung, M., Migliavacca, M., Mu, M.,
866 Saatchi, S., Santoro, M., Thurner, M., Weber, U., Ahrens, B., Beer, C., Cescatti, A.,
867 Randerson, J. T., and Reichstein, M.: Global covariation of carbon turnover times with
868 climate in terrestrial ecosystems, *Nature*, 51, 213–217,
869 <https://doi.org/10.1038/nature13731>, 2014.

870 Christian, H. J., Blakeslee, R. J., Boccippio, D. J., Boeck, W. L., Buechler, D. E., Driscoll,
871 K. T., Goodman, S. J., Hall, J. M., Koshak, W. J., Mach, D. M., and Stewart, M. F.:
872 Global frequency and distribution of lightning as observed from space by the Optical
873 Transient Detector, *J. Geophys. Res-Atmos.*, 108, ACL 4-1-ACL 4-15,
874 <https://doi.org/10.1029/2002JD002347>, 2003.

875 Costa, L.: Nutrient enrichment changes water transport structures of savanna woody plants,
876 figshare, <https://doi.org/10.6084/m9.figshare.13252052.v1>, 2020.

877 Cramer, W., Bondeau, A., Woodward, F. I., Prentice, I. C., Betts, R. A., Brovkin, V., Cox,
878 P. M., Fisher, V., Foley, J. A., Friend, A. D., Kucharik, C., Lomas, M. R., Ramankutty,
879 N., Sitch, S., Smith, B., White, A., and Young-Molling, C.: Global response of terrestrial
880 ecosystem structure and function to CO₂ and climate change: Results from six dynamic
881 global vegetation models, *Glob. Change Biol.*, 7, 357–373,
882 <https://doi.org/10.1046/j.1365-2486.2001.00383.x>, 2001.

883 de Camargo, M. G. G., de Carvalho, G. H., Alberton, B. D. C., Reys, P., and Morellato, L.
884 P. C.: Leafing patterns and leaf exchange strategies of a cerrado woody community.
885 *Biotropica*, 50, 442–454. <https://doi.org/10.1111/btp.12552>, 2018.

886 D'Onofrio, D., Baudena, M., Lasslop, G., Nieradzik, L. P., Wårlind, D., and von
887 Hardenberg, J.: Linking vegetation-climate-fire relationships in Sub-Saharan Africa to
888 key ecological processes in two dynamic global vegetation models, *Fr. Environ. Sci.*, 8,
889 <https://doi.org/10.3389/fenvs.2020.00136>, 2020.

890 de Queiroz, L.P., Cardoso, D., Fernandes, M.F., Moro, M.F: Diversity and Evolution of
891 Flowering Plants of the Caatinga Domain., In: Silva, J.M.C., Leal, I.R., Tabarelli, M.
892 (eds) *Caatinga*. Springer-Cham, https://doi.org/10.1007/978-3-319-68339-3_2, 2017.

893 Drüke, M., Forkel, M., von Bloh, W., Sakschewski, B., Cardoso, M., Bustamante, M.,
894 Kurths, J., and Thonicke, K.: Improving the LPJmL4-SPITFIRE vegetation–fire model
895 for South America using satellite data, *Geosci. Model Dev.*, 12, 5029–5054,
896 <https://doi.org/10.5194/gmd-12-5029-2019>, 2019.

897 Feron, S., Cordero, R. R., Damiani, A., MacDonell, S., Pizarro, J., Goubanova, K.,
898 Valenzuela, R., Wang, C., Rester, L., and Beaulieu, A.: South America is becoming
899 warmer, drier, and more flammable. *Commun. Earth Environ.*, 5, 501,
900 <https://doi.org/10.1038/s43247-024-01654-7>, 2024.

901 Forkel, M., Carvalhais, N., Schaphoff, S., V. Bloh, W., Migliavacca, M., Thurner, M., and
902 Thonicke, K.: Identifying environmental controls on vegetation greenness phenology
903 through model–data integration. *Biogeosciences*, 11, 7025–7050.
904 <https://doi.org/10.5194/bg-11-7025-2014>, 2014.

905 Gomes, L., Miranda, H. S., and Bustamante, M. M. C.: How can we advance the knowledge
906 on the behavior and effects of fire in the Cerrado biome? *Forest Ecol. Manag.*, 417, 281–
907 290. <https://doi.org/10.1016/j.foreco.2018.02.032>, 2018.

908 Gomes, L., Miranda, H. S., Soares-Filho, B., Rodrigues, L., Oliveira, U., and Bustamante,
909 M. M. C.: Responses of plant biomass in the Brazilian savanna to frequent fires, *Front.*
910 *Forest Glob. Change*, 3, 507710. <https://doi.org/10.3389/ffgc.2020.507710>, 2020a.

911 Gomes, L., Miranda, H. S., Silvério, D. V., and Bustamante, M. M. C.: Effects and
912 behaviour of experimental fires in grasslands, savannas, and forests of the Brazilian
913 Cerrado, *Forest Ecol. Manag.* 458, 117804.
914 <https://doi.org/10.1016/j.foreco.2019.117804>, 2020b.

915 Gomes, L., Schüler, J., Silva, C., Alencar, A., Zimbres, B., Arruda, V., Silva, W. V. da,
916 Souza, E., Shimbo, J., Marimon, B. S., Lenza, E., Fagg, C. W., Miranda, S., Morandi, P.
917 S., Marimon-Junior, B. H., and Bustamante, M.: Impacts of fire frequency on net CO₂
918 emissions in the Cerrado savanna vegetation, Fire, 7, 208,
919 <https://doi.org/10.3390/fire7080280>, 2024.

920 Grimm, A. M., Vera, C. S., and Mechoso, C. R.: The South American monsoon system,
921 In: The Global Monsoon System: Research and Forecast, WMO/TD 1266, TMRP
922 Rep. 70, 219–238, Available at <https://core.ac.uk/download/pdf/36730348.pdf>, 2005.

923 Guglielmo, M., Tang, F. H. M., Pasut, C., and Maggi, F.: SOIL-WATERGRIDS,
924 mapping dynamic changes in soil moisture and depth of water table from 1970 to
925 2014, Scient. Data, 8, 263. <https://doi.org/10.1038/s41597-021-01032-4>, 2021.

926 Hengl, T., Walsh, M. G., Sanderman, J., Wheeler, I., Harrison, S. P., and Prentice, I. C.:
927 Global mapping of potential natural vegetation: An assessment of machine learning
928 algorithms for estimating land potential, PeerJ, 6, e5457,
929 <https://doi.org/10.7717/peerj.5457>, 2018.

930 Hersbach, H., Bell, B., Berrisford, P., Hirahara, S., Horányi, A., Muñoz-Sabater, J., Nicolas, J., Peubey, C., Radu, R., Schepers, D., Simmons, A., Soci, C., Abdalla, S., Abellán, X., Balsamo, G., Bechtold, P., Biavati, G., Bidlot, J., Bonavita, M., ... Thépaut, J. N. (2020). The ERA5 global reanalysis. *Quarterly Journal of the Royal Meteorological Society*, 146, 1999–2049. <https://doi.org/10.1002/qj.3803>
931
932
933
934

935 Hoffmann, W. A., Adasme, R., Haridasan, M., T. De Carvalho, M., Geiger, E. L., Pereira,
936 M. A. B., Gotsch, S. G., and Franco, A. C.: Tree topkill, not mortality, governs the
937 dynamics of savanna–forest boundaries under frequent fire in central Brazil, Ecology,
938 90, 1326–1337, <https://doi.org/10.1890/08-0741.1>, 2009.

939 Hoffmann, W. A., da Silva, E. R., Machado, G. C., Bucci, S. J., Scholz, F. G., Goldstein,
940 G., and Meinzer, F. C.: Seasonal leaf dynamics across a tree density gradient in a
941 Brazilian savanna, Oecologia, 145, 306–315, <https://doi.org/10.1007/s00442-005-0129-x>, 2005.

942

943 Hoffmann, W. A., Orthen, B., and Franco, A. C.: Constraints to seedling success of savanna
944 and forest trees across the savanna-forest boundary, *Oecologia*, 140, 252–260,
945 <https://doi.org/10.1007/s00442-004-1595-2>, 2004.

946 Hofmann, G., Cardoso, M., Alves, R., Weber, E., Barbosa, A., De Toledo, P., Pontual, F.,
947 Salles, L., Hasenack, H., Passos Cordeiro, J. L., Aquino, F., and Oliveira, L.: The
948 Brazilian Cerrado is becoming hotter and drier, *Glob. Change Biol.*, 27,
949 <https://doi.org/10.1111/gcb.15712>, 2021.

950 IBGE: Brazilian Vegetation, Available at
951 <https://www.ibge.gov.br/en/geosciences/maps/state-maps/19470-brazilian-vegetation.html?andt=downloads>, 2017.

953 IBGE: Biomas e Sistema Costeiro-Marinho do Brasil—PGI, Available at
954 <https://www.ibge.gov.br/apps/biomas/#/home>, 2024.

955 Jackson, R. B., Canadell, J., Ehleringer, J. R., Mooney, H. A., Sala, O. E., and Schulze, E.
956 D.: A global analysis of root distributions for terrestrial biomes, *Oecologia*, 108, 389–
957 411. <https://doi.org/10.1007/BF00333714>, 1996.

958 Klein Goldewijk, K., Beusen, A., Drecht, G., and Vos, M.: The HYDE 3.1 spatially explicit
959 database of human-induced global land-use change over the past 12,000 years, *Global
960 Ecol Biogeogr.*, 20, 73–86, <https://doi.org/10.1111/j.1466-8238.2010.00587.x>, 2011.

961 Langan, L., Higgins, S. I., and Scheiter, S.: Climate-biomes, pedo-biomes or pyro-biomes:
962 which world view explains the tropical forest–savanna boundary in South America? *J.
963 Biogeogr.*, 44, 2319–2330, <https://doi.org/10.1111/jbi.13018>, 2017.

964 Lehmann, C. E. R., Anderson, T. M., Sankaran, M., Higgins, S. I., Archibald, S., Hoffmann,
965 W. A., Hanan, N. P., Williams, R. J., Fensham, R. J., Felfili, J., Hutley, L. B., Ratnam,
966 J., San Jose, J., Montes, R., Franklin, D., Russell-Smith, J., Ryan, C. M., Durigan, G.,
967 Hiernaux, P., ... Bond, W. J.: Savanna vegetation-fire-climate relationships differ among
968 continents. *Science*, 343, 548–552, <https://doi.org/10.1126/science.1247355>, 2014.

969 Machida, W. S., Gomes, L., Moser, P., Castro, I. B., Miranda, S. C., da Silva-Júnior, M.
970 C., and Bustamante, M. M. C.: Long term post-fire recovery of woody plants in

971 savannas of central Brazil, Forest Ecol. Manag., 493, 119255.
972 <https://doi.org/10.1016/j.foreco.2021.119255>, 2021.

973 Malhi, Y., Aragão, L. E. O. C., Galbraith, D., Huntingford, C., Fisher, R., Zelazowski, P.,
974 Sitch, S., McSweeney, C., and Meir, P.:Exploring the likelihood and mechanism of a
975 climate-change-induced dieback of the Amazon rainforest, P. Natl. A. Sci., 106, 20610–
976 20615, <https://doi.org/10.1073/pnas.0804619106>, 2009.

977 MapBiomass 9.0: MapBiomass Uso e Cobertura 9.0, Available at
978 <https://brasil.mapbiomas.org/colecoes-mapbiomas/>, 2024.

979 MapBiomass Fogo: MapBiomass Fogo 3.0, Available at
980 <https://mapbiomasfogocol3v1.netlify.app/index.html>, 2024.

981 [MapBiomass Fogo: MapBiomass Fogo 4.0, Available at https://brasil.mapbiomas.org/wp-](https://brasil.mapbiomas.org/wp-content/uploads/sites/4/2025/06/Fact_Fogo_colecao4.pdf)
982 [content/uploads/sites/4/2025/06/Fact_Fogo_colecao4.pdf, 2025.](https://brasil.mapbiomas.org/wp-content/uploads/sites/4/2025/06/Fact_Fogo_colecao4.pdf)

983 Martens, C., Hickler, T., Davis-Reddy, C., Engelbrecht, F., Higgins, S. I., Von Maltitz, G.
984 P., Midgley, G. F., Pfeiffer, M., and Scheiter, S.: Large uncertainties in future biome
985 changes in Africa call for flexible climate adaptation strategies, Glob. Change Biol., 27,
986 340–358 <https://doi.org/10.1111/gcb.15390>, 2021.

987 MCTI: Quarto inventário nacional de emissões e remoções antrópicas de gases de efeito
988 estufa setor uso da terra, mudança do uso da terra e florestas, Available at:
989 <https://repositorio.mcti.gov.br/handle/mctic/4782>, 2020.

990 MCTI: First biennial transparency report of Brazil to the United Nations Framework
991 Convention on Climate Change, Available at: [https://www.gov.br/mcti/pt-](https://www.gov.br/mcti/pt-br/acompanhe-o-mcti/sirene/publicacoes/relatorios-bienais-de-transparencia-btrs)
992 [br/acompanhe-o-mcti/sirene/publicacoes/relatorios-bienais-de-transparencia-btrs](https://www.gov.br/mcti/pt-br/acompanhe-o-mcti/sirene/publicacoes/relatorios-bienais-de-transparencia-btrs), 2024.

993 Moncrieff, G. R., Scheiter, S., Langan, L., Trabucco, A., and Higgins, S. I.: The future
994 distribution of the savannah biome: model-based and biogeographic contingency, Philos.
995 T. R. Soc. B., 371, 20150311, <https://doi.org/10.1098/rstb.2015.0311>, 2016.

996 Myers, N., Mittermeier, R. A., Mittermeier, C. G., da Fonseca, G. A. B., and Kent, J.:
997 Biodiversity hotspots for conservation priorities, Nature, 403, 853–858.
998 <https://doi.org/10.1038/35002501>, 2000.

999 Oberhagemann, L., Billing, M., Von Bloh, W., Drüke, M., Forrest, M., Bowring, S. P. K.,
1000 Hetzer, J., Ribalaygua Batalla, J., and Thonicke, K.: Sources of uncertainty in the global
1001 fire model SPITFIRE: development of LPJmL-SPITFIRE1.9 and directions for future
1002 improvements, *Geosci. Model Dev.*, 18, 2021-2025, <https://doi.org/10.5194/gmd-18-2021-2025>, 2025.

1004 Oliveira, R. S., Bezerra, L., Davidson, E. A., Pinto, F., Klink, C. A., Nepstad, D. C., and
1005 Moreira, A.: Deep root function in soil water dynamics in cerrado savannas of central
1006 Brazil. *Funct. Ecol.*, 19, 574–581, <https://doi.org/10.1111/j.1365-2435.2005.01003.x>,
1007 2005.

1008 Oliveira, U., Soares-Filho, B., de Souza Costa, W. L., Gomes, L., Bustamante, M., and
1009 Miranda, H.: Modeling fuel loads dynamics and fire spread probability in the Brazilian
1010 Cerrado, *Forest Ecol. Manag.*, 482, 118889,
1011 <https://doi.org/10.1016/j.foreco.2020.118889>, 2021.

1012 Oliver, T. H., Heard, M. S., Isaac, N. J. B., Roy, D. B., Procter, D., Eigenbrod, F.,
1013 Freckleton, R., Hector, A., Orme, C. D. L., Petchey, O. L., Proença, V., Raffaelli, D.,
1014 Suttle, K. B., Mace, G. M., Martín-López, B., Woodcock, B. A., and Bullock, J. M.:
1015 Biodiversity and resilience of ecosystem functions. *Trends Ecol. Evol.*, 30, 673–684,
1016 <https://doi.org/10.1016/j.tree.2015.08.009>, 2015.

1017 Peel, M. C., Finlayson, B. L., and McMahon, T. A.: Updated world map of the Köppen-
1018 Geiger climate classification, *Hydrol. Earth Syst. Sc.*, 11, 1633–1644,
1019 <https://doi.org/10.5194/hess-11-1633-2007>, 2007.

1020 Perkins, O., Kasoar, M., Voulgarakis, A., Smith, C., Mistry, J., and Millington, J. D. A.
1021 (2024). A global behavioural model of human fire use and management: WHAM! v1.0,
1022 *Geosci. Model Dev.*, 17, 3993–4016, <https://doi.org/10.5194/gmd-17-3993-2024>, 2024.

1023 Pivello, V. R.: The Use of fire in the Cerrado and amazonian rainforests of Brazil: past and
1024 present. *Fire Ecol.*, 7, 24-39. <https://doi.org/10.4996/fireecology.0701024>, 2011.

1025 Ratnam, J., Bond, W. J., Fensham, R. J., Hoffmann, W. A., Archibald, S., Lehmann, C. E.
1026 R., Anderson, M. T., Higgins, S. I., and Sankaran, M.: When is a ‘forest’ a savanna, and

1027 why does it matter? *Global Ecol. Biogeogr.*, 20, 653–660. <https://doi.org/10.1111/j.1466-8238.2010.00634.x>, 2011.

1029 Ribeiro, J., and Walter, B.: As principais fitofisionomias do bioma Cerrado In: Sano, S.M.,
1030 Almeida, S.P. and Ribeiro, J.F. (Eds.), *Cerrado Ecologia e Flora*, p. 152–212., 2008.

1031 Rodrigues, A. A., Macedo, M. N., Silvério, D. V., Maracahipes, L., Coe, M. T., Brando, P.
1032 M., Shimbo, J. Z., Rajão, R., Soares-Filho, B., and Bustamante, M. M. C.: Cerrado
1033 deforestation threatens regional climate and water availability for agriculture and
1034 ecosystems, *Glob. Change Biol.*, 28, 6807–6822, <https://doi.org/10.1111/gcb.16386>,
1035 2022.

1036 Ronquim, C. C., Prado, C. H. B. de A., and de Paula, N. F.: Growth and photosynthetic
1037 capacity in two woody species of cerrado vegetation under different radiation
1038 availability, *Braz. Arch. Biol. Techn.*, 46, 243–252, <https://doi.org/10.1590/S1516-89132003000200016>, 2003.

1040 Saboya, P., and Borghetti, F.: Germination, initial growth, and biomass allocation in three
1041 native Cerrado species, *Braz. J. Bot.*, 35, 129–135, <https://doi.org/10.1590/S0100-84042012000200002>, 2012.

1043 Sakschewski, B., Von Bloh, W., Boit, A., Rammig, A., Kattge, J., Poorter, L., Peñuelas, J.,
1044 and Thonicke, K.: Leaf and stem economics spectra drive diversity of functional plant
1045 traits in a dynamic global vegetation model, *Glob. Change Biol.*, 21, 2711–2725,
1046 <https://doi.org/10.1111/gcb.12870>, 2015.

1047 Sakschewski, B., von Bloh, W., Drüke, M., Sörensson, A. A., Ruscica, R., Langerwisch, F.,
1048 Billing, M., Bereswill, S., Hirota, M., Oliveira, R. S., Heinke, J., and Thonicke, K.:
1049 Variable tree rooting strategies are key for modelling the distribution, productivity and
1050 evapotranspiration of tropical evergreen forests. *Biogeosciences*, 18, 4091–4116,
1051 <https://doi.org/10.5194/bg-18-4091-2021>, 2021.

1052 Salazar, A., Katzfey, J., Thatcher, M., Syktus, J., Wong, K., and McAlpine, C.:
1053 Deforestation changes land–atmosphere interactions across South American biomes,
1054 *Global Planet. Change*, 139, 97–108, <https://doi.org/10.1016/j.gloplacha.2016.01.004>,
1055 2016.

1056 Sano, E. E., Rodrigues, A. A., Martins, E. S., Bettoli, G. M., Bustamante, M. M. C., Bezerra,
1057 A. S., Couto, A. F., Vasconcelos, V., Schüler, J., and Bolfe, E. L.: Cerrado ecoregions:
1058 A spatial framework to assess and prioritize Brazilian savanna environmental diversity
1059 for conservation, *J. Environ. Manage.*, 232, 818–828,
1060 <https://doi.org/10.1016/j.jenvman.2018.11.108>, 2019.

1061 Schaphoff, S., Von Bloh, W., Rammig, A., Thonicke, K., Biemans, H., Forkel, M., Gerten,
1062 D., Heinke, J., Jägermeyr, J., Knauer, J., Langerwisch, F., Lucht, W., Müller, C.,
1063 Rolinski, S., and Waha, K.: LPJmL4 – a dynamic global vegetation model with managed
1064 land – Part 1: Model description. *Geosci. Model Dev.*, 11, 1343–1375,
1065 <https://doi.org/10.5194/gmd-11-1343-2018>, 2018.

1066 Scholz, F. G., Bucci, S. J., Goldstein, G., Meinzer, F. C., Franco, A. C., and Salazar, A.:
1067 Plant- and stand-level variation in biophysical and physiological traits along tree density
1068 gradients in the Cerrado, *Braz. J. Plant Physiol.*, 20, 217–232,
1069 <https://doi.org/10.1590/S1677-04202008000300006>, 2008.

1070 Schüler, J.: Áreas prioritárias para a restauração no Cerrado: aumentando os benefícios e
1071 reduzindo os conflitos, Masters dissertation, Universidade de Brasília, 105 p. Available
1072 at <http://repositorio.unb.br/handle/10482/39518>, 2020.

1073 Schüler, J., and Bustamante, M. M. C.: Spatial planning for restoration in Cerrado:
1074 Balancing the trade-offs between conservation and agriculture, *J. Appl. Ecol.*, 59, 2616–
1075 2626, <https://doi.org/10.1111/1365-2664.14262>, 2022.

1076 Schumacher, V., Setzer, A., Saba, M. M. F., Naccarato, K. P., Mattos, E., and Justino, F.:
1077 Characteristics of lightning-caused wildfires in central Brazil in relation to cloud-ground
1078 and dry lightning. *Agr. Forest Meteorol.*, 312, 108723,
1079 <https://doi.org/10.1016/j.agrformet.2021.108723>, 2022.

1080 Shinozaki, K., Yoda, K., Hozumi, K., and Kira, T.: A quantitative analysis of plant form-
1081 the Pipe Model Theory: II. Further evidence of the theory and its application in forest
1082 ecology. *Jpn. J. Ecol.*, 14, 133–139. https://doi.org/10.18960/seitai.14.4_133, 1964.

1083 Simon, M. F., and Pennington, T.: Evidence for adaptation to fire regimes in the tropical
1084 savannas of the Brazilian Cerrado, *Int. J. Plant Sci.*, 173, 711–723,
1085 <https://doi.org/10.1086/665973>, 2012.

1086 Solbrig, O. T., Medina, E., and Silva, J. F.: *Biodiversity and savanna ecosystem processes: A global perspective* (Vol. 121). Springer, 1996.

1088 Souchie, F. F., Pinto, J. R. R., Lenza, E., Gomes, L., Maracahipes-Santos, L., and Silvério,
1089 D. V.: Post-fire resprouting strategies of woody vegetation in the Brazilian savanna, *Acta
1090 Bot. Bras.*, 31, 260–266, <https://doi.org/10.1590/0102-33062016abb0376>, 2017.

1091 Souza, C. R. D., Coelho De Souza, F., Françoso, R. D., Maia, V. A., Pinto, J. R. R., Higuchi,
1092 P., Silva, A. C., Prado Júnior, J. A. D., Farrapo, C. L., Lenza, E., Mews, H., Rocha, H.
1093 L. L., Mota, S. L., Rodrigues, A. L. C., Silva-Sene, A. M. D., Moura, D. M., Araújo, F.
1094 D. C., Oliveira, F. D., Gianasi, F. M., ... Santos, R. M. D.: Functional and structural
1095 attributes of Brazilian tropical and subtropical forests and savannas, *Forest Ecol. Manag.*,
1096 558, 121811, <https://doi.org/10.1016/j.foreco.2024.121811>, 2024.

1097 Strassburg, B. B. N., Brooks, T., Feltran-Barbieri, R., Iribarrem, A., Crouzeilles, R., Loyola,
1098 R., Latawiec, A. E., Oliveira Filho, F. J. B., Scaramuzza, C. A. de M., Scarano, F. R.,
1099 Soares-Filho, B., and Balmford, A.: Moment of truth for the Cerrado hotspot, *Nat. Ecol.
1100 Evol.*, 1, 1–3, <https://doi.org/10.1038/s41559-017-0099>, 2017.

1101 Swann, A. L. S., Longo, M., Knox, R. G., Lee, E., and Moorcroft, P. R.: Future deforestation
1102 in the Amazon and consequences for South American climate, *Agr. Forest Meteorol.*,
1103 214–215, 12–24, <https://doi.org/10.1016/j.agrformet.2015.07.006>, 2015.

1104 Syktus, J. I., and McAlpine, C. A.: More than carbon sequestration: Biophysical climate
1105 benefits of restored savanna woodlands, *Sci. Rep-UK*, 6, 29194,
1106 <https://doi.org/10.1038/srep29194>, 2016.

1107 Terra, M. C. N. S., Nunes, M. H., Souza, C. R., Ferreira, G. W. D., Prado-Junior, J. A. do,
1108 Rezende, V. L., Maciel, R., Mantovani, V., Rodrigues, A., Morais, V. A., Scolforo, J. R.
1109 S., and Mello, J. M.: The inverted forest: Aboveground and notably large belowground
1110 carbon stocks and their drivers in Brazilian savannas, *Sci. Total Environ.*, 867, 161320,
1111 <https://doi.org/10.1016/j.scitotenv.2022.161320>, 2023.

1112 Terra, M. D. C. N. S., Santos, R. M. D., Prado Júnior, J. A. D., De Mello, J. M., Scolforo,
1113 J. R. S., Fontes, M. A. L., Schiavini, I., Dos Reis, A. A., Bueno, I. T., Magnago, L. F. S.,
1114 and Ter Steege, H.: Water availability drives gradients of tree diversity, structure and
1115 functional traits in the Atlantic–Cerrado–Caatinga transition, Brazil, *J. Plant Ecol.*, 11,
1116 803–814, <https://doi.org/10.1093/jpe/fty017>, 2018.

1117 Thonicke, K., Billing, M., von Bloh, W., Sakschewski, B., Niinemets, Ü., Peñuelas, J.,
1118 Cornelissen, J. H. C., Onoda, Y., van Bodegom, P., Schaepman, M. E., Schneider, F. D.,
1119 and Walz, A.: Simulating functional diversity of European natural forests along climatic
1120 gradients, *J Biogeogr.*, 47, 1069–1085, <https://doi.org/10.1111/jbi.13809>, 2020.

1121 Thonicke, K., Spessa, A., Prentice, I. C., Harrison, S. P., Dong, L., and Carmona-Moreno,
1122 C.: The influence of vegetation, fire spread and fire behavior on biomass burning and
1123 trace gas emissions: Results from a process-based model, *Biogeosciences*, 7, 1991–2011,
1124 <https://doi.org/10.5194/bg-7-1991-2010>, 2010.

1125 Tumber-Dávila, S. J., Schenk, H. J., Du, E., and Jackson, R. B.: Plant sizes and shapes above
1126 and belowground and their interactions with climate, *New Phytol.*, 235, 1032–1056,
1127 <https://doi.org/10.1111/nph.18031>, 2022.

1128 van der Werf, G. R., Randerson, J. T., Giglio, L., van Leeuwen, T. T., Chen, Y., Rogers, B.
1129 M., Mu, M., van Marle, M. J. E., Morton, D. C., Collatz, G. J., Yokelson, R. J., and
1130 Kasibhatla, P. S.: Global fire emissions estimates during 1997–2016, *Earth Syst. Sci.
1131 Data*, 9, 697–720, <https://doi.org/10.5194/essd-9-697-2017>, 2017.

1132 Von Bloh, W., Schaphoff, S., Müller, C., Rolinski, S., Waha, K., and Zaehle, S.:
1133 Implementing the nitrogen cycle into the dynamic global vegetation, hydrology, and crop
1134 growth model LPJmL (version 5.0), *Geosci. Model Dev.*, 11, 2789–2812,
1135 <https://doi.org/10.5194/gmd-11-2789-2018>, 2018.

1136 Whitley, R., Beringer, J., Hutley, L. B., Abramowitz, G., De Kauwe, M. G., Evans, B.,
1137 Haverd, V., Li, L., Moore, C., Ryu, Y., Scheiter, S., Schymanski, S. J., Smith, B., Wang,
1138 Y.-P., Williams, M., and Yu, Q.: Challenges and opportunities in land surface modelling
1139 of savanna ecosystems, *Biogeosciences*, 14, 4711–4732, <https://doi.org/10.5194/bg-14-4711-2017>, 2017.

1141 Wirth, S. B., Braun, J., Heinke, J., Ostberg, S., Rolinski, S., Schaphoff, S., Stenzel, F., von
1142 Bloh, W., Taube, F., and Müller, C.: Biological nitrogen fixation of natural and
1143 agricultural vegetation simulated with LPJmL 5.7.9, *Geosci. Model Dev.*, 17, 7889–
1144 7914, <https://doi.org/10.5194/gmd-17-7889-2024>, 2024.

1145 Wullschleger, S. D., Epstein, H. E., Box, E. O., Euskirchen, E. S., Goswami, S., Iversen, C.
1146 M., Kattge, J., Norby, R. J., van Bodegom, P. M., and Xu, X.: Plant functional types in
1147 Earth system models: Past experiences and future directions for application of dynamic
1148 vegetation models in high-latitude ecosystems, *Ann. Bot-London*, 114, 1–16.
1149 <https://doi.org/10.1093/aob/mcu077>, 2014.

1150 Zemp, D. C., Schleussner, C.-F., Barbosa, H. M. J., Hirota, M., Montade, V., Sampaio, G.,
1151 Staal, A., Wang-Erlandsson, L., and Rammig, A.: Self-amplified Amazon forest loss due
1152 to vegetation-atmosphere feedbacks, *Nature Commun.*, 8, 14681,
1153 <https://doi.org/10.1038/ncomms14681>, 2017.